# The Regulation of Mfn1-Mediated Mitochondrial Outer Membrane Fusion

Jennifer Martínez Bocanegra

A dissertation

submitted in partial fulfillment of the

requirements for the degree of

Doctor of Philosophy

University of Washington

2025

Reading Committee:

Suzanne Hoppins, Chair

Dana Miller

Michael Ailion

Program Authorized to Offer Degree:

Biochemistry

University of Washington

## Abstract

The Regulation of Mfn1-Mediated Mitochondrial Outer Membrane Fusion

Jennifer Martínez Bocanegra

Suzanne Hoppins

Department of Biochemistry

Mitochondria are often depicted in textbooks as static organelles whose principal purpose is to power cells; however, they are constantly moving and morphing shape in response to cellular requirements which go beyond the energetic needs of the cell. The dynamic properties exhibited by mitochondria include transport and positioning via interactions with cytoskeleton, and fission and fusion of the mitochondrial membranes, all of which are critical for maintaining mitochondrial function. The implications of disrupted mitochondrial transport and division have been extensively described in comparison to disrupted mitochondrial fusion. However, both mitochondrial fission and fusion are required to maintain a balanced and healthy network of mitochondria able to effectively respond to cellular demands. Mitochondrial fission and fusion are mediated by large GTPases from the Dynamin Superfamily of Proteins. Mitochondrial outer membrane fusion is mediated in mammals by the paralogs Mfn1 and Mfn2, collectively known as the mitofusins. Mutations in *MFN2* are the cause for the most common form of Charcot-Marie-Tooth Type 2A Disease (CMT2A), though the mechanistic relationship between dysfunction of mitochondrial outer membrane fusion and the presentation of symptoms in patients with CMT2A has not been previously investigated. The following work describes the use of two biochemically characterized Mfn1 variants, Mfn1 S329P and Mfn1 S228A, to further investigate how mitofusin function is regulated and how regulation of Mfn1 contributes to cellular function. First, I present the use of the

nematode *Caenorhabditis elegans* as a powerful new model to understand the contribution of Mfn1 S329P to neuronal dysfunction. This variant, along with its homologous disease-associated variant Mfn2 S350P, are fusion incompetent and exhibit phenotypes when expressed in cells that include redistribution of mitochondria to the perinuclear region. Mfn1 S329P was expressed in *C. elegans* and neuronal function was assessed by measuring neuron-dependent behaviors. Transgenic worms expressing Mfn1 S329P exhibited uncoordinated locomotion and decreased progeny that was likely due to an egg-laying defect. To better understand how mitofusin dysfunction contributes to disease, I performed genetic screens for suppressors of the behavioral phenotypes. Given that a candidate-based approach did not yield insight into the cellular functions contributing to the behavioral defects, I performed an unbiased genetic screen to identify candidates. I isolated *agns-1 (um0017)* in *C. elegans* and describe the formation of Mfn1 S329P associated mitochondrial clusters in neurons, which is facilitated by *agns-1*. Finally, I propose leveraging *C. elegans* as a tractable model for investigating how CMT2A-associated mitofusin variants contribute to neuronal dysfunction in real-time. In the following chapter I investigate the functional impacts of phosphorylation at Mfn1 S228 with respect to cellular health. I find that blocking phosphorylation of Mfn1 S228 renders cells slightly more susceptible to cell death induced by the ATP synthase inhibitor Oligomycin. Taken together, I demonstrate that dysregulation of Mfn1 contributes to cellular dysfunction and provide a novel model that bridges the gap between our understanding of mitofusin function *in vitro.*

**Table of Contents**

**Table of Figures**

**Acknowledgements**

I have infinite gratitude for all those who helped me along this way, from Mrs. McDonald and Mrs. McCloud, my Kindergarten teachers, to my PhD advisor, Dr. Suzanne Hoppins. I am especially grateful for my committee and for all the support I have received throughout my training. I thank Dr. Dana Miller and Dr. Michael Ailion for providing me the space and resources to continue growing as a scientist, and Dr. Irini Topalidou for the guidance and support. Thanks to Nick for always making sure I had NGM plates, and thanks to Drs. Stephanie Sloat, Amy Bounds, and Sophie Hurwitz for following me down and allowing me to join them through numerous rabbit holes. A major thanks to Dr. Giovanna Guerrero Medina, Dr. Monica Feliu Mojer, and Dr. Omar Quintero for modeling healthy work behaviors, fostering my personal and professional growth, and constantly inspiring me to be a better scientist and human being. Finally, **THIS WORK AND THESE FINDINGS WERE MADE POSSIBLE BY FUNDING FROM THE NATIONAL SCIENCE FOUNDATION AND THE NATIONAL INSTITUTES OF HEALTH.**

Scientific progress is critical for improving quality of life of all living beings on the planet. These institutions not only provide funding for critical research projects but also ensure that scientific findings are disseminated, and ethical practices are maintained. Without these organizations, the future of ethical science and healthcare is at risk. *Fight in defiance, embrace science.*

**Dedication**

*Para las almas abandonadas, los reclusos, los que sueñan con mundos que no existen*

*Para los que conocieron el hambre, la pobreza, la soledad y el duelo*

*Para los ojos que han visto tragedias y sufrimiento*

*y aun así no han perdido la compasión.*

*Esta obra es para todos los que han experimentado lo más profundo de la vida y, en oposición a la maldad, en un acto de rebeldía, deciden amar incondicionalmente.*

*“We are not made up, as we had always supposed, of successively enriched packets of our own parts. We are shared, rented, occupied. At the interior of our cells, driving them, providing the oxidative energy that sends us out for the improvement of each shining day, are the mitochondria, and in a strict sense they are not ours. They turn out to be little separate creatures, the colonial posterity of migrant prokaryocytes, probably primitive bacteria that swam into ancestral precursors of our eukaryotic cells and stayed there. Ever since, they have maintained themselves and their ways, replicating in their own fashion, privately, with their own DNA and RNA quite different from ours. They are as much symbionts as the rhizobial bacteria in the roots of beans. Without them, we would not move a muscle, drum a finger, think a thought. Mitochondria are stable and responsible lodgers, and I choose to trust them.”*

-Lewis Thompson, “The Lives of a Cell”

# Chapter 1. Introduction

## 1.1 Mitochondria and Cellular Homeostasis

Life in its most basic form is a cell, a complex and diverse network of evolutionarily conserved systems working in concerted effort to maintain homeostasis. Each component contributes to this effort in one or multiple ways, as we have learned since Robert Hooke first reported the microscopic structure of plant tissues in the 17th century, though it wasn't until the 19th century that our view and understanding of the mechanisms that drive life began to come into focus. During the mid 1800's, biochemistry emerged as a term for a discipline of science that combined biology and chemistry. Contemporary to the emergence of biochemistry as a field, Albert von Kölliker would be the first to report the existence of what he described as "granules" in the muscle tissue of insect wings. It wasn't until the late 1800's, however, that these granules would have a proper name: mitochondria, meaning thread granules. During the late 1950's it was found that mitochondria are the primary site for energy production and were therefore labeled the powerhouse of the cell by Philip Siekevitz who popularized the term among English-speaking countries. Since then, our understanding of the cellular functions of mitochondria have grown to include roles beyond ATP generation.

Mitochondria are double membrane bound organelles containing an outer mitochondrial membrane (OMM) separated from an inner mitochondrial membrane (IMM) by an intermembrane space. The IMM contains invaginations called cristae, which extend into the mitochondrial matrix. Cristae provide the surface area where Oxidative Phosphorylation occurs, leading to the production of energy in the form of ATP. Mitochondria contain their own genome which codes for 13 protein components of Oxidative Phosphorylation and is enclosed in nucleoids that are housed within the mitochondrial matrix. The ATP generated from Oxidative Phosphorylation is then used to power a multitude of cellular pathways, including cytokinesis and synaptic transmission, among others. In addition to its role in energy metabolism, mitochondria also maintain intracellular calcium levels, regulate the programmed response to cell death, and are involved in pathways associated with the immune response (Angajala et al., 2018; Mehta, Weinberg, & Chandel, 2017).

To effectively function in cells, mitochondria form networks that are highly dynamic, constantly rearranging their distribution and morphology in response to cellular demands (Fenton, Jongens, & Holzbaur, 2021). Within its lifetime, a cell will undergo drastic changes in mitochondrial morphology and distribution. The adaptable response of mitochondria to cellular cues is maintained by dynamic properties including organelle trafficking, fission and fusion (Chan, 2020; Morris & Hollenbeck, 1993). Mitochondria are highly motile organelles, moving in response to cellular signals that direct their positioning to various sites, such as those with high energy demand or where calcium buffering is required (Chada & Hollenbeck, 2003; Verburg & Hollenbeck, 2008). Mitochondria are transported and positioned where required through associations with the cytoskeleton which are facilitated by adaptor protein complexes that link mitochondria to trafficking motor proteins (Fransson, Ruusala, & Aspenström, 2003; MacAskill, Brickley, Stephenson, & Kittler, 2009; Stowers, Megeath, Górska-Andrzejak, Meinertzhagen, & Schwarz, 2002; van Spronsen et al., 2013).

Mitochondria accommodate for the broad range of cellular demands by responding to cellular cues with morphological changes that facilitate the required function. These dynamic processes are highly regulated by various cellular signaling pathways. At steady state, mitochondrial fission and fusion are balanced, and typically this is reflected in a mitochondrial network composed of tubules of variable sizes distributed throughout the cell. This balance can be tuned in response to cellular cues to favor mitochondrial fission, leading to a fragmented network of small, spherical mitochondria, or in favor of mitochondrial fusion leading, to a stringy, interconnected network of mitochondria. During the cell cycle, for example, mitochondrial networks will fragment to facilitate equal distribution of mitochondria into daughter cells. During the G1/S phase, however, mitochondria form a highly interconnected, hyperfused network leading to an increase in energy production required to power DNA replication (Mishra & Chan, 2014). Mitochondrial health and quality control also heavily rely on dynamic mitochondrial properties. For example, fragmentation of mitochondria facilitates removal of damaged organelles through selective mitochondrial autophagy (Narendra, Tanaka, Suen, & Youle, 2008). On the other hand, fusion of mitochondria enables content mixing and diffusion of damaged mitochondrial components and provides protection against starvation-induced stress through a mechanism that involves an increase in cristae and ATP production. (Legros, Fréderic; Lombès, Anne; Frachon, Paule; Rojo, 2002; Rambold, Kostelecky,

Elia, & Lippincott-Schwartz, 2011; Tondera et al., 2009). The vastly different morphological responses to homeostatic perturbations highlight the importance of both mitochondrial fission and fusion in quality control and cellular health (Hales & Fuller, 1997; Jimah & Hinshaw, 2019). Indeed, disruptions in the function of the protein players that facilitate mitochondrial dynamic properties of transport, fission and fusion have been reported in a plethora of diseases including cardiac myopathies, cancers, neuropathies and neurodegenerative disorders.

### 1.2 Mechanisms of Mitochondrial Membrane Fusion

Membrane fusion is an energy demanding process composed generally of three major steps: 1) tethering of opposing membranes, 2) formation of docking complexes that bring membranes closer together, and finally 3) lipid mixing and fusion of membranes. This simplified model does not account for all the individual players and events that need to occur to meet the energetic requirement of fusing membranes. While fusion of smaller vesicles such as dense core vesicles or synaptic vesicles relies mainly on SNARE proteins guided by small Ras-GTPases, membrane remodeling of larger organelles such as the ER and mitochondria is mediated by GTPases from the dynamin superfamily of proteins (DSP). These proteins harness GTP binding and hydrolysis to couple conformational changes and oligomerization with membrane remodeling (Ramachandran & Schmid, 2018). conformational changes and oligomerization with membrane remodeling (Ramachandran & Schmid, 2018). Reshaping mitochondria includes sequential remodeling of the OMM and IMM, presenting a unique energetic requirement. The machines doing the work have been identified, yet multiple questions remain. For example, it’s unclear what facilitates tethering, whether tethering occurs in a particular assembly state, how mitochondrial fusion progresses from a state where opposing membranes are close together, to a fully fused lipid bilayer, and what happens to the fusion complexes after membrane fusion.

#### 1.2.1 Membrane Remodeling by Dynamin Superfamily Proteins

Mitochondrial membrane fission and fusion are coordinated processes that are facilitated by different DSPs through highly conserved domains. The GTPase domain is the most conserved domain within the DSP. DSPs ability to remodel membranes relies on binding of GTP in the nucleotide binding pocket and hydrolysis-driven conformational changes that reshape the membrane. However, the affinity

for nucleotide in DSP is much lower in comparison to Ras family GTPases, and the intrinsic rate of GTP hydrolysis is higher in DSPs. Therefore, unlike small Ras GTPases, DSPs don't necessitate GTPase-activating proteins (GAPs) or guanine exchange factors (GEFs) to regulate hydrolysis. The GTPase domain in DSP's is composed of four consensus elements, G1-G4. The phosphate-binding P loop is in the G1 motif, while the G2 and G3 coordinate with Mg2+ to facilitate hydrolysis, and the G4 motif binds the nucleotide base. The G-domains of DSPs form an intermolecular interface in a nucleotide-dependent manner and the nucleotide state is stabilized, stimulating GTP hydrolysis. A distinguishing feature among DSPs is the ability to form higher order structures. In fission DSPs, a stalk containing a GTPase effector domain (GED) facilitates higher order assembly, while helical bundles (HB) containing heptad repeats compose facilitate assembly of most fusion DSPs. The least conserved domain within DSPs is the membrane-binding domain, which targets the corresponding DSP to its associated membrane (Jimah & Hinshaw, 2019).

In vertebrates, mitochondrial fission is mediated by the DSP Drp-1, which is recruited to the OMM by MFF, MiD49/51 (Losó n, Song, Chen, & Chan, 2013; Otera et al., 2010; Palmer et al., 2011). OMM and IMM fusion are facilitated by different DSP's. OMM fusion is mediated by the mammalian paralogs Mfn1 and Mfn2, collectively known as the mitofusins; while IMM fusion requires Opa-1 (H. Chen et al., 2003; Ge et al., 2020).

### 1.2.2 Mitofusin-Mediated Mitochondrial Membrane Fusion

The mitofusin paralogs share conserved features with Opa-1 and other DSPs, including an N-terminal GTPase domain, helical bundles, and a membrane-targeting domain(s). The use of truncated mitofusin constructs has shed light on the mechanistic contributions each domain plays in OMM fusion, though a complete model for mitofusin-mediated OMM fusion has yet to be described. What is currently understood is that each domain within the mitofusins contributes to effective fusion of the OMM, as do each individual mitofusin paralog Mfn1 and Mfn2. This is evidenced by work demonstrating that mitochondrial fusion is most efficient when Mfn1 and Mfn2 form heterotypic complexes on opposing membranes, indicating that the mitofusin paralogs have some unique functions in membrane fusion (S. R. Sloat, Whitley, Engelhart, & Hoppins, 2019). To enable membrane fusion, the mitofusins form oligomers

both in a single membrane, or in cis, and across two membranes, or in trans. Both mitofusins contain two alpha helical bundles (HB1& HB2), a GTPase domain, and a transmembrane domain. GTP binding permits the formation of an intermolecular interface by the GTPase domain, called the G-G interface, which triggers GTP hydrolysis. The formation of the G-G interface between mitofusins on separate membranes tethers the mitochondria together and represents the first step in membrane fusion. Beyond this, it's unclear how tethered but separate mitochondria progress to a mitochondrion with a fully fused lipid bilayer.

### 1.3 Mitochondrial Distribution in Cells

Mitochondrial movement and positioning are coordinated processes that rely on signaling molecules, the cytoskeleton, trafficking motor proteins, and motor-mitochondrial adaptor complexes. Different changes in these components or their regulation can lead to redistribution of the mitochondrial network through various mechanisms that may be related. Dysfunctional microtubule-based mitochondrial transport resulting in preferential nucleus-directed transport can lead to an accumulation of mitochondria to the perinuclear region. The perinuclear redistribution of mitochondria has also been observed in mutant mitofusin cell lines. Additionally, defective mitochondrial transport has been reported in cell lines expressing disease-associated mitofusin variants, directly implicating the mitofusins in microtubule transport of mitochondria. Other mechanisms for preferential perinuclear positioning of mitochondria include the tethering of mitofusins to the nuclear envelope, which has been previously reported and a tether identified in yeast. (Dorn, 2020; Stephanie R Sloat & Hoppins, 2022; Zervopoulos et al., 2022). These possibilities are not mutually exclusive, multiple factors may be contributing independently or together to facilitate this aberrant mitochondrial redistribution.

#### 1.3.1 Mitochondrial Cytoskeletal Adaptors

The associations between mitochondria and the cytoskeleton are highly dynamic and are facilitated by various proteins. Originally reported in flies, Milton, and its mammalian homologuesTRAK1 and TRAK2, interact with cytoskeletal motors on microtubules and actin and are recruited to mitochondria by Miro. Miro proteins are atypical Rho GTPases that contain two GTPase domains flanking two Ca2+ binding domains, followed by a C-terminal transmembrane domain that targets the protein to the OMM

(Fransson, Ruusala, & Aspenström, 2003; Fransson et al., 2006). The N-terminal GTPase domain is the most structurally similar of these domains to other Rho GTPases and appears to facilitate Miro's roles in mitochondrial dynamics (Babic et al., 2015; K. Davis, Basu, Izquierdo-Villalba, Shurberg, & Schwarz, 2023). Expression of a constitutively active N-terminal GTPase mutation in Miro causes a redistribution of the mitochondrial network to the perinuclear region in non-neuronal cells, though the mechanism for this drastic rearrangement is unclear (Schuler et al., 2017). Miro proteins bind to Ca2+ through EF hands and this inhibits mitochondrial transport, thus indicating that Miro GTPases not only regulate the interaction between mitochondria and the cytoskeleton, but also mitochondrial distribution (Brickley & Stephenson, 2011; Guo et al., 2005; MacAskill, Rinholm, et al., 2009; Russo et al., 2009; Saotome et al., 2008). Miro proteins have also been reported to complex with Metaxins in dendritic mitochondria to form complexes that link mitochondria to microtubule motors in a TRAK-independent manner (Zhao et al., 2021). Depletion of Miro, however, does not abolish anterograde mitochondrial transport, and TRAK proteins are reported to associate with the OMM in Miro knockout cells (López-Doménech et al., 2018). Therefore, it is likely that there are additional players facilitating interactions between mitochondria and the cytoskeleton and regulating mitochondrial transport.

### 1.3.2 The MMA Connection: Mitochondria, Microtubules, and Actin

Mitochondrial movement is an art, a beautifully choreographed dance with a purpose. Processive transport of mitochondria is polarized, bidirectional, and occurs via interactions with microtubules and microtubule-associated motors. Trafficking toward the cell periphery in an anterograde direction is facilitated by Kinesin-1, also known as KIF5 (**KI**nesin **F**amily member **5**). Mutant KIF5b isoforms are reported to cause a collapse of mitochondria to the perinuclear region, further supporting the role of Kinesin in anterograde transport of mitochondria (K. Tanaka, Sugiura, Ichishita, Mihara, & Oka, 2011; Y. Tanaka et al., 1998). Retrograde transport of mitochondria on microtubules is facilitated by the motor Dynein, which carries various cargo toward the nucleus.

Mitochondria have long been known to associate with actin as well as microtubules to mediate mitochondrial transport (Boldogh & Pon, 2006; Hollenbeck & Saxton, 2005; Huang et al., 1999; Moore & Holzbaur, 2018). Mitochondria in budding yeast travel on actin, however early evidence for this in

vertebrates came from experiments documenting the changes in mitochondrial transport velocities of neurons grown under conditions where actin or microtubules were depolymerized. Mitochondria in neurons treated with cytochalasin D to depolymerize actin exhibited increase transport velocity compared to untreated; while the mitochondria in neurons treated with nocodazole to block polymerization of microtubules traveled at much slower velocities compared to untreated (Morris & Hollenbeck, 1995). This early work suggested a role for microtubules in processive transport, and further work supported this by demonstrating that actin-binding Myosin protein activity slows down mitochondrial transport (Pathak, Sepp, & Hollenbeck, 2010). A few Myosin proteins have been implicated in mitochondrial transport. Depletion of Myosin V or VI increased mitochondrial velocities in a bidirectional or retrograde manner, respectively, though these do not directly bind to mitochondria. A novel class of Myosin, Myosin XIX, is the only known Myosin to associate directly with both mitochondria and actin. Myosin XIX binds the OMM via a direct interaction with its C-terminal MyMoMA domain (Bocanegra et al., 2019; Hawthorne, Mehta, Singh, Wong, & Quintero, 2016; Quintero et al., 2009).

Miro proteins stabilize Myosin XIX, facilitating insertion of the MyMoMa domain to the OMM. Myosin XIX has been implicated in mitochondrial dynamics including balancing fission-fusion events (Bocanegra, Adikes, & Quintero, 2020; Moore, Wong, Simpson, & Holzbaur, 2016). Actin plays a role in mitochondrial division by facilitating assembly of Drp-1 and further constriction of the membranes and has recently been reported to be present at sites of mitochondrial fusion (Gatti, Schiavon, Cicero, Manor, & Germain, 2024).

### 1.4 Mitofusin Dysfunction and Disease

Altered mitochondrial dynamics are implicated indirectly and directly with disease. In mice, loss of either *MFN1* or *MFN2* results in embryonic lethality (H. Chen et al., 2003). Decreased expression of MFN2 is associated with poor prognoses in several different cancers (Ahn, Li, Zhang, & Hyun, 2018; You et al., 2021). In addition, mutations in *MFN2* are associated with several diseases, including heart disease, diabetes, and neuropathies (Y. Chen, Liu, & Dorn, 2011; Dai & Jiang, 2019; Sebastián et al., 2012). Mutations in *MFN2*, but not *MFN1*, are most frequently the cause of the peripheral neuropathy

Charcot-Marie-Tooth Syndrome type 2A (CMT2A) (Detmer & Chan, 2007; Feely et al., 2011; Kijima et al., 2005).

### 1.4.1 Charcot-Marie-Tooth Disease

CMT are a group of several neuropathies caused by mutations in different genes, many of which are associated with mitochondria and mitochondrial dynamics (Soh et al., 2020). Most of the mutations are autosomal dominant and appear to cause deterioration of neuromuscular function. CMT2A is the most common inherited peripheral motor neuropathy and is characterized by progressive distal muscle weakness and atrophy, deformities and poor gait (Feely et al., 2011). CMT2A-associated *MFN2* mutations have been reported in essentially every domain of the protein, though the majority can be found within or near the GTPase domain (Filadi, Pendin, & Pizzo, 2018; Yan et al., 2018). Symptoms can vary from mild to severe among patients, with little correlation between domain function and disease-associated mutation. For example, Mfn2 R364 is a conserved residue located between the HB1 and G-domain that has several reported variations. Patients expressing R364W or R364P exhibit severe, early onset of symptoms; while the R364Q variant is associated with moderate, late onset of symptoms. All CMT2A-associated Mfn2 R364 variants were reported to exhibit increased GTPase activity when expressed in cells, however this alone is insufficient to explain the progression and intensity of symptoms in patients expressing the variant (Li et al., 2019). The different presentations in disease pathology among patients with variations in the same Mfn2 domains is not fully understood. This highlights the need for novel models to bridge the gap between our understanding of how biochemical perturbations and cellular phenotypes observed in cells expressing CMT2A variants translate to symptom severity.

### 1.4.2 Modeling mitofusin-associated pathology

Mitofusin associated pathology is generally associated with neuromuscular dysfunction and sensory neuropathy. It has been shown that when mitochondria are trapped around the nucleus, rather than positioned in axonal sites where they are needed, neuronal function is compromised (Morris & Hollenbeck, 1993; Rawson et al., 2014; Ruthel & Hollenbeck, 2003). Locomotor defects indicative of neuronal dysfunction have been reported in fly and mouse models of CMT2A. However, current models of CMT2A lack the tools to observe mitochondrial dynamics in living cells and the real-time impact on

locomotor function and other neuronal-associated behaviors. Given that CMT2A is a neuropathy and mitochondrial transport has the greatest effect in neurons, such a model would yield great insights into the progression of CMT2A from the biochemical mechanisms to physiological impacts.

## Chapter 2. *agns-1* facilitates mitochondrial clustering in a Mitofusin model of disease

### Abstract

In this study, we develop an *in vivo* model of CMT2A and assess neuronal function. Expression of Mfn1 S329P under a neuronal promoter produces an uncoordinated locomotion phenotype and decreased progeny in *C. elegans*, consistent with impaired neuronal function in these animals. This phenotype was not suppressed in the absence of various mitochondrial quality control or trafficking proteins. A genetic screen for suppressors of the neuronal-associated behaviors identified *C. elegans d2045.8 (um0017).* Images of neuronal mitochondria revealed a mitochondrial clustering phenotype in transgenic Mfn1 S329P worms, which was partially suppressed by mutant *d2045.8 (um0017).* We henceforth refer to *d2045.8* as **AG**gregatio**N S**eparator, or *agns-1*. In summary, we identify a novel gene linking mitochondrial fusion and redistribution in disease-associated mitofusin variants and propose the use of *C. elegans* as a model for studying mitochondrial fusion in health and disease.

## 2.1 Introduction

Neurons are especially sensitive to disruptions in mitochondrial dynamics due to their high energy demand and distinct cell shape and polarity. The unique morphological properties of neurons require mitochondria to travel to and from various cellular compartments and adapt their shape to meet their specialized metabolic requirements. Transport of healthy mitochondria over long distances in neurons, from the axon to the growth cone or synapse, is critical for powering neuronal growth and function (Chada & Hollenbeck, 2003; Ruthel & Hollenbeck, 2003; Verburg & Hollenbeck, 2008). Depletion of healthy pools of mitochondria in neuronal compartments such as the presynaptic terminals leads to neuronal degeneration, reinforcing the significance of these dynamic mitochondrial properties in maintaining neuronal health (Kleele et al., 2021; Mandal & Drerup, 2019; Ruthel & Hollenbeck, 2003).

A growing interest has been placed on the genes and protein products associated with mitochondrial fusion. Outer mitochondrial membrane (OMM) and inner mitochondrial membrane (IMM) fusion are both mediated by different proteins from the same family: FZO-1/Mfn 1/2 and EAT-3/Opa1, respectively. Proteins associated with OMM and IMM fusion are highly conserved across species, in mammals, the paralogs Mfn1 and Mfn2, collectively known as the mitofusins, are both required for efficient fusion of the OMM. Interestingly, mutations in *MFN2*, but not *MFN1*, are the cause of the most common form of Charcot-Marie-Tooth disease, CMT2A (Feely et al., 2011; Kijima et al., 2005; Soh et al., 2020). CMT2A is a neuromuscular disorder that primarily affects the peripheral nerves, causing progressive muscle deterioration. Redistribution of the mitochondrial network to the perinuclear region and defective mitochondrial transport have been observed in models carrying CMT2A-associated mutations in *MFN2* (Baloh, Schmidt, Pestronk, & Milbrandt, 2007). *In vitro* studies of CMT2A-associated and other mitofusin variants that exhibit perinuclear aggregation of the mitochondrial network have provided mechanistic insight into the fusogenic function of mitofusins. Recently, a biochemical analysis of the CMT2A-associated variant Mfn2 S350P, and its homologous variant, Mfn1 S329P revealed hypertethering of mitochondria by mitofusins to be a cause for the mitochondrial aggregation (Stephanie R. Sloat & Hoppins, 2023). However, the mechanisms behind preferential distribution to the perinuclear region, and the general contribution of this abnormal phenotype to the neuromuscular symptoms reported in CMT2A patients remains unclear.

In this study, we expressed murine Mfn1 S329P in the *C. elegans* nervous system under the control of the pan-neuronal Rab-3 promoter. We analyzed the behavioral response of worms carrying the mutant transgene as a measure of neuronal dysfunction, then performed a genetic screen for suppression of the associated neuronal phenotypes. We identify *C. elegans d2045.8* as a novel gene associated with the mutant *MFN1* behavioral phenotypes. Furthermore, analysis of neuronal mitochondria in *C. elegans* touch neurons revealed a mitochondrial phenotype that is also suppressed, supporting a causative link between mitofusin dysfunction and neuromuscular function. Our data indicate that *C. elegans* is a novel and tractable model to study functional characteristics of mitofusins and their implications in neuronal cellular health and behavior.

## 2.2 Results

### 2.2.1 Expression of CMT2A-associated Mitofusin variant in *C. elegans*. disrupts neuronal function

Mitofusin function is conserved among eukaryotes. The two mammalian mitofusin paralogs, Mfn1 and Mfn2, share high homology and domain conservation across species including yeast Fzo1, *Drosophila* Marf, and *C. elegans* FZO-1 (Rojo, Legros, Chateau, & Lombès, 2002). ). CMT2A-afflicted patients' exhibit symptoms of neuropathy including impaired motor function that result in muscle weakness, atrophy and poor gait. Motor defects and neurodegeneration have also been observed in fly, worm and mouse mitofusin null or disease models, though the relationship between mitofusin fusion function and neurodegeneration are less clear (Byrne et al., 2019). We have made strides in understanding the mechanisms behind mitofusin function primarily by exploiting mitofusin disease-associated variants to dissect the mechanisms of mitofusin-mediated OMM remodeling (Samanas, Engelhart, & Hoppins, 2020). To better understand how mitofusin CMT2A-associated variant phenotypes in cells relate to overall physiology and behavior, we expressed a well-characterized variant of Mfn1 in *C. elegans* neurons and assayed for behaviors associated with neuronal dysfunction. Specifically, we chose the variant Mfn1 S329P, which is homologous to the CMT2A-associated variant Mfn2 S350P. Characterization of both proline variants in mammalian cells revealed a dramatic redistribution of mitochondria to the perinuclear region, and aggregation of the mitochondrial network resulting from abnormal mitochondrial tethering (Stephanie R. Sloat & Hoppins, 2023).

We expressed the human MFN1 S329 variant pan neuronal promoter, prab-3 (Nguyen et al., 2016). The transgene also included a nuclear GFP reporter to confirm that it was expressed. Locomotion and egg-laying circuits are coordinated processes in *C. elegans* that require proper neuronal function. We initially observed an uncoordinated locomotion phenotype in two stably expressing transgenic Mfn1 S329P lines, consistent with previously reported expression of CMT2A associated mutations in the Drosophila Marf gene (El Fissi et al., 2018). To quantify this, we counted the number of body bends per minute in comparison to N2 Bristol strain (WT) and observed impaired locomotion in both transgenic Mfn1 S329P *C. elegans* lines assayed (Fig 2.1A). Specifically, worms appeared to be dragging the tail and lifting their heads higher as they moved. A notable decrease in progeny was also observed in worms

expressing Mfn1 S329P during the peak egg-laying stages compared to WT N2 worms not expressing (Fig 2.1B). The decrease in progeny is likely a consequence stemming from defective egg-laying, as suggested by the significant decrease in eggs laid / hour in Mfn1 S329P worms (Fig 2.1C). However, when accounting for total progeny including larva observed over four days, the difference in progeny was not as striking as in eggs laid/hour. Additionally, accumulation of hatched larvae within the parent, known as bagging, was consistently seen among Mfn1 S329P transgenic worms resulting in early mortality compared to WT (Fig 2.1D). The locomotion and egg-laying phenotypes observed in worms are consistent with expression of Mfn1 S329P disrupting neuronal function. Further, this is similar with the locomotor defects reported in flies expressing CMT2A-associated mutations in the *MFN2* homologue, MARF. Together, this indicates that *C. elegans* is also a tractable model that can be leveraged to improve our understanding of how mitofusin dysfunction contributes to neuronal dysfunction and disease progression.

### 2.2.2 Mitochondrial trafficking and quality control genes linked to Mitofusins are not required for the behavioral phenotypes observed in Mfn1 S329P transgenic worms

Depletion of axonal mitochondria by impairing anterograde mitochondrial transport has been noted to cause neurodegeneration (Rawson et al., 2014; Sure et al., 2018). The motors that enable the polarized transport of mitochondria on microtubules are Kinesin, which steers mitochondrial transport in an anterograde direction, and Dynein directing transport in retrograde, or toward the nucleus (Glater, Megeath, Stowers, & Schwarz, 2006; Schnapp & Reese, 1989; Y. Tanaka et al., 1998). Attachment of mitochondria to Kinesin and Dynein is a regulated process that is facilitated through an adaptor complex, which links the organelle to the cytoskeleton. Miro proteins are atypical Rho GTPases that bind to mitochondria through their C terminal domain, whereas the N terminal GTPase domain of Miro proteins play an important role in maintaining mitochondrial distribution (Fransson, Ruusala, & Aspenström, 2006). Miro recruits Trafficking Kinesin Protein 1 (TRAK1), which binds to Kinesin and Dynein. Together, Miro and TRAK proteins form an adaptor complex that facilitates regulation of bidirectional mitochondrial transport by associating with the molecular motors that steer the movement (Brickley & Stephenson, 2011; López-Doménech et al., 2018; Stowers et al., 2002).

Both mitofusins have been reported to interact with the Miro/ TRAK complex, and defective mitochondrial transport has been observed in neurons of *MFN2* knock-out mice and in cultured neurons expressing Mfn2 CMT2A-associated mutations (Baloh et al., 2007; A. Misko, Jiang, Wegorzewska, Milbrandt, & Baloh, 2010; A. L. Misko, Sasaki, Tuck, Milbrandt, & Baloh, 2012). Interestingly, constitutive activation of the first GTPase domain in Miro-1 also leads to a redistribution of the mitochondrial network to the perinuclear region, though the clusters do not appear as compressed as those observed in cells expressing the Mfn1 S329P variant (Fransson et al., 2003; Stephanie R. Sloat & Hoppins, 2023). To determine whether disruptions in mitochondrial transport could be contributing to the behavioral phenotype associated with Mfn1 S329P, we crossed worms expressing Mfn1 S329P to worms with null or loss-of-function alleles of the mitochondrial transport adaptors *miro-1 (tm1966)* and *trak-1*, as well as the retrograde motor dynein homologue, *dhc-1 (or283ts).* We then assayed for suppression of the uncoordinated locomotion phenotype (Fig 2.2A). Consistent with previously reported data from our lab, preferential retrograde transport of mitochondria was not driving the observed behavioral phenotypes (Stephanie R. Sloat & Hoppins, 2023).

Clearance of damaged mitochondria in cells occurs through a specific form of autophagy termed mitophagy. Stabilization of the kinase Pink-1 on the OMM recruits Parkin/PDR-1, an E3 ligase that targets Mfn2 and other proteins on the OMM for degradation (Y. Chen & Dorn, 2013; Yang et al., 2008). Adaptor proteins recognize the targeted proteins and initiate autophagosome formation. Removal of OMM targets and fragmentation of the mitochondrial network facilitate engulfment by the autophagosome, which then fuses with the lysosome where the remaining organelle will then be degraded. Mutations in Pink-1 and Parkin are linked to Parkinson's disease and neurodegeneration, and overexpression of Pink-1 and Parkin also results in perinuclear clustering of mitochondria (Vives-Bauza et al., 2010). We therefor considered the possibility that dysfunctional Pink-1 / Parkin-mediated mitophagy could be involved in the cellular mechanism that causes the Mfn1 S329P-associated neuronal phenotypes. We again generated double mutants by crossing worms expressing Mfn1 S329P with null-mutants of *pink-1 (tm1779)* or *pdr-1 (gk348738).* Neither showed suppression of the uncoordinated locomotion observed in both transgenic lines expressing Mfn1 S329P alone, suggesting that neither Pink-1 nor Parkin function is required for the mutant Mfn1 S329P locomotion phenotype in worms (Fig 2.2B).

### 2.2.3 A forward genetic screen identifies genes required for Mfn1 S329P mutant behavioral phenotype

Given that the candidate genes surveyed did not suppress the locomotion phenotype, we decided to take an unbiased approach to identify genes required for the behavioral phenotype observed in Mfn1 S329P mutant worms by performing a forward genetic screen. EMS was used to mutagenize transgenic Mfn1 S329P worms, and the subsequent F2 generations were assessed for suppression of locomotion phenotype. Twelve isolates that appeared to have differences in locomotion compared to Mfn1 S329P worms alone were initially identified. *um0015, um0017, um0024,* and *um0031* all suppressed the Mfn1 S329P uncoordinated locomotion as measure by body bends per minute, whereas *um0032* appeared to enhance this phenotype (Fig 2.3A). Notably, some isolates appeared to have improved locomotion by eye, though it was not significant when quantified, possibly due to different uncoordinated locomotive behaviors. *um0017* and *um0024* appeared similar in phenotype; in addition to suppressing the uncoordinated locomotion both exhibited a mildly protruding vulval phenotype when isolated away from the MFN1 S329P transgene. In this study, we describe the characterization of *um0017*.

In addition to changes in locomotion, we noted that Mfn1 S329P worms had fewer progeny compared to WT, likely due to an egg-laying defect. Given that egg-laying and locomotor behaviors in *C. elegans* are coordinated by serotonergic command neurons and cholinergic motor neurons, we reasoned that egg-laying may also be affected in Mfn1 S329P worms in a neuronal dependent manner. We quantified egg-laying and found that mutant *um0017* also suppressed the defect observed in both Mfn1 S329P worm lines assayed (Fig 2.3B).

### 2.2.4 Mitochondria form clusters in the PLM neurons of Mfn1 S329P transgenic worms

Perinuclear clustering of mitochondria has been observed in cell lines expressing CMT2A-associated mitofusin variants (Baloh et al., 2007). Previous work investigating the Mfn1 S329P / Mfn2 S350P variant also showed a striking redistribution of the mitochondria to the perinuclear region upon induced expression in cells. Biochemical analysis demonstrated that Mfn1 S329P / Mfn2 S350P variants do not support mitochondrial fusion, and that the accumulation of mitochondria is principally due to

hypertethering of organelles (Stephanie R. Sloat & Hoppins, 2023). We posited that if the behavioral phenotype observed in worms expressing the Mfn1 S329P variant is due to abnormalities in mitochondrial morphology or mitochondrial aggregation, then we should be able to observe such a phenotype in neurons. To test our hypothesis, we expressed the outer mitochondrial membrane protein tomm20 fused with mCherry under the control of the MEC-7 promoter to enable visualization of mitochondria (Fig 2.4A). We chose to look specifically at the PLM neuron given it's easily identified and observed various puncta throughout the PLM neuron in both WT and transgenic Mfn1 S329P expressing worms, noting the presence of seemingly larger puncta in neurons of Mfn1 S329P worms. To quantify distribution of mitochondria throughout the neurons, a line was traced over the puncta starting 100μM away from the soma through the length of the entire axon. The fluorescence intensity values from each individual pixel generated a line profile of mitochondrial distribution and fluorescence intensity throughout the axon. Worms expressing Mfn1 S329P exhibited more sequential pixels with high fluorescence intensity corresponding to the locations where mitochondrial aggregates were observed in the respective image (Fig 2.4B). To determine if *um0017* suppressed the mitochondrial phenotypes observed in Mfn1 S329P worms, we generated line scan profiles of *um0017* ; Mfn1 S329P and observed fewer cluster-like puncta than in the Mfn1 S329P strains (Fig 2.4). Together, this suggests that *um0017* suppresses the neuronal phenotypes associated with expression of Mfn1 S329P in worms through a mechanism that involves changes in mitochondrial shape and distribution.

### 2.2.5 Identification of *d2045.8* as a suppressor of Mfn1 S329P-associated neuronal phenotypes

*um0017* was backcrossed to WT and among the progeny were observed animals that appeared to move similar to WT, others that exhibited uncoordinated locomotion consistent with Mfn1 S329P, and a population of worms with a distinct phenotype from WT, Mfn1 S329P worms, or *um0017 ;* Mfn1 S329P worms. Such animals appeared shorter than either WT or Mfn1 S329P expressing worms, less active, and had a striking protruding vulval phenotype. To determine if this new phenotype was linked to the suppressor mutation, a population was isolated and mated back to two Mfn1 S329P worm lines. The F2 generations were scored, and it was noted that within the plates scored, 43% – 62% exhibited a mild vulval phenotype but appeared to have improved locomotion compared to Mfn1 S329P alone, while 24% - 30% exhibited the dramatic protruding vulval phenotype associated with *um0017* alone. Thus, the

protruding vulval phenotype appears to be linked to *um0017*. The suppressor mutation was subsequently mapped to Chromosome III between genetic positions -11 and 12 by monitoring co-segregation of the phenotype with fluorescent markers integrated at known positions on each chromosome in the strains EG8040 and EG8041 (Table I).

To determine the gene identity of *um0017*, we compared whole genome sequencing of the *um0017*; *prab-3::Mfn1S329P* double mutant and *um0017* mutant alone to N2 Bristol. We focused on G:C to A:T transition mutations most consistent with EMS, were located within the mapped region, and affected genes that were conserved in mammals. These criteria produced a shortlist of fewer than 10 gene candidates. We generated double mutants with Mfn1 S329P to evaluate whether candidates would phenocopy um0017. Uncoordinated locomotion was not suppressed when the transgene was combined with *vps-53*, which visibly appeared more sluggish, or *clip-1* (Fig 2.5A). Another candidate may prove to be more promising: *d2045.8*, which is located on Chromosome III, Genomic position: III 10482288 - 10483943 (1655 cM). The results from our whole genome sequencing identified a point mutation in the strains containing um0017 that is predicted to cause a premature stop at C63* in exon-1. We found another variant of *d2045.8* in the Million Mutant Project strains (Waterston et al., 2013); *d2045.8 (gk348738)* contains a mutation predicted to cause a premature stop at position Q207*. *um0017* and *d2045.8(gk348738)* were mated to WT and to themselves, and the phenotypes were followed. *um0017* heterozygotes presented a mildly protruding vulval phenotype when compared to homozygous *um0017* mutants. We also observed a protruding vulval phenotype in *d2045.8 (gk348738)* animals, though with less penetrance as *um0017* heterozygotes and much less striking than *um0017* homozygotes. The progeny of *um0017* heterozygotes mated to *d2045.8 (gk348738)* presented with a vulval phenotype or no vulval phenotype. Therefore, it was difficult to determine whether these mutations are allelic. However, mating *d2045.8 (gk348738)* heterozygotes produced an F1 progeny in which close to half the animals scored exhibited a mild vulval phenotype consistent with *um0017* heterozygotes; while the remaining exhibited a more striking protruding vulva. Together, this suggests that the *um0017* allele may be linked to *d2045.8*.

## 2.3 Discussion

In this study, we expressed the biochemically characterized murine mitofusin variant Mfn1 S329P in *C. elegans* and report locomotor defects consistent with neuronal dysfunction. We performed both candidate and forward genetic screens for suppressors of the phenotype and have identified a novel gene, *d2045.8*, as a contributor (P. Davis et al., 2022). We report that worms expressing the Mfn1 S329P variant specifically in neurons exhibit locomotor deficiencies. Although this is not the first time that locomotor defects related to the expression of mitofusin variants have been reported, it is the first instance in which a mammalian variant that has previously been biochemically characterized is expressed in an invertebrate organism. Through a genetic search for suppressors of the uncoordinated movement of transgenic animals, we have isolated a new allele of *d2045.8 (um0017)*. The *um0017* allele alone exhibits a protruding vulval phenotype, uncoordinated locomotion, and a decrease in progeny with an observed increase in sterility. *um0017* is predicted to coordinate a premature stop, and this mutation was sufficient to suppress the locomotor defects observed in two transgenic lines. In addition, we demonstrated the presence of mitochondrial aggregates in neurons of transgenic worms expressing Mfn1 S329P. The formation of such aggregates is reduced in the absence of the suppressor gene; therefore, we have named this gene **Ag**gregatio**n S**uppressor **1**, or *agns-1*. We suggest that the organism should be given greater attention as a model for investigating the links between the biochemical functions of mitofusins, the cellular phenotypes associated with these variants, and the effect on neuronal function and behavior as it pertains to disease.

Over 100 different mutations in *MFN2* have been reported in CMT2A patients. Given the GTP requirement for efficient OMM fusion, the GTP binding and turnover have been investigated for several CMT2A-associated mitofusin variants. Variants within the G-domain that have been assayed exhibit vastly different GTP binding and turnover rates, ranging from mildly decreased to significantly increased.. (Li et al., 2019). In addition to changes in enzymatic activity, mitochondrial clustering and transport defects have also been reported in fibroblasts expressing CMT2A-associated Mfn2 variants. Mfn2 R94 is located between the GTPase domain and HB1 and several variants have been reported in this position, including Mfn2 R94Q and R94W. Both of these Mfn2 CMT2A-associated variants exhibit increased GTPase activity and form mitochondrial clusters when expressed in cells, although the clusters appear

more compressed in R94W (Baloh et al., 2007; Detmer & Chan, 2007). Mfn2 T105 is in the G interface, and the CMT2A-associated Mfn2 T105M also exhibits increased GTPase activity and causes mitochondrial aggregation when expressed in cells. Mfn2 R94 and Mfn2 T105 are both conserved residues, yet the pathogenesis in CMT2A-associated Mfn2 R94Q is early onset and severe, whereas Mfn2 T105M is late onset, and presents with mild symptoms. Mfn2 R94 and Mfn2 T105 variants are reported to be fusion deficient, though the mechanism behind the block in mitofusin function has not been fully described. Further, the relationship between the biochemical analysis of enzyme activity, the phenotypes observed in cells, and the disease prognosis has not been investigated in detail. Expression of either variant Mfn1 S329P or Mfn1 S350P interferes with the function of WT mitofusins, resulting in a loss of mitofusin-mediated fusogenic ability in cell models and in vitro. The expression of this variant also leads to a massive redistribution of the mitochondrial network to the perinuclear region. However, aggregate formation alone is not sufficient in explaining the preferential distribution to the perinuclear region, nor does it relate to the neurodegenerative effects observed in CMT2A patients. Here, we have shown that the presence of mitochondrial aggregates associated with Mfn1 S329P expression is indeed a contributing factor to the neuronal dysfunction, and likely the pathogenesis observed in CMT2A patients.

Sloat and Hoppins demonstrated that the aggregation of the mitochondrial network in cells expressing Mfn1 S329P / Mfn2 S350P is due to mitofusin complexes becoming tethered without the ability to progress to complete mitochondrial fusion (Stephanie R. Sloat & Hoppins, 2023). Dynein knock-down did not impede mitochondrial cluster formation, and we have now confirmed in an organism that preferential retroactive transport is not the primary cause for behavioral phenotypes associated with Mfn1 S329P expression. It was somewhat surprising to find that none of the known mitochondrial transport components are required for the formation of large mitochondrial clusters. One explanation for this is that Miro proteins appear to play independent regulatory roles in mitochondrial dynamics. It is noteworthy that in mammals there are two Miro proteins, Miro 1 and Miro 2; and two TRAK proteins, TRAK 1 and TRAK 2 (Fransson et al., 2006). In the worm, there are three genes sharing homology with Miro proteins, although a couple of them have been suggested to be pseudogenes. There is at least one study to the contrary, but it remains to be seen whether, indeed, a single gene and isoform in worms exhibits all the functions that Miro 1 and Miro 2 exhibit in mammals. Recent findings from studies in mammalian cells have

revealed independent functions for Miro 1/2 and TRAK 1/2 in facilitating mitochondrial transport and dynamics.

A BLAST analysis indicates that *agns-1* shares homology with BTB domain-containing proteins of the *KCTD* family, particularly *KCTD* 10. The family is not specific to nematodes as they exist throughout the animal kingdom and are associated with processes including protein quality control systems, among others. The mammalian ortholog is expressed in fibroblasts as well as in peripheral nerves, consistent with the models used for the study of Mfn1 S329P. *KCTD* proteins consist of a family with conserved N' Bric-a-brack, Tram-track, Broad complex (BTB) domain (AKA POZ domain). BTB/POZ domain proteins perform a variety of cellular processes, including in cell progression, apoptosis, cytoskeletal dynamics and protein transport. Several BTB/POZ domain proteins are associated with protein ubiquitination and de-ubiquitination actingas adaptors for ubiquitin-mediated degradation. Originally named due to their homology to potassium channels, it is now understood that KCTD proteins are not potassium channels. KCTD proteins are divided into groups, with KCTD10 under Group B. Downstream targets of other members of this group are associated with degradation of Rho proteins and have been reported to interact with Cul3. Together, this suggests that protein quality control pathways may be facilitating the aggregation of mitochondria in Mfn1 S329P variants. Interestingly, a genetic screen looking for substrates of E3 ubiquitin ligases important for myoblast fusion identified the mammalian *KCTD10* and a couple of its targets. Among these proteins were several involved in actin nucleation, and it was suggested that KCTD10 targets those proteins to dismantle actin structures post-myoblast fusion (Rodríguez-Pérez et al., 2021). *agns-1* had not previously been associated with mitofusins, therefore, it would be surprising if mitofusins were a direct target. To gain further insight into potential roles or associations between *agns-1* and mitofusin, we screened various public databases of reported interactors in common. Among them, *stip-1* and *marc-5* stood out due to their associations with mitochondrial morphology and protein quality control pathways. Mammalian Stip 1 is a cochaperone for Hsp70 and Hsp90 which is reported to facilitate handing off protein targets between heat shock proteins. Changes in mitochondrial morphology have been reported in mutants of yeast *stip-1* homolog Sti1, and it was suggested that Sti1 facilitates transfer of protein precursors to mitochondria in a mechanism involving HSP70 (Hoseini et al., 2016).

A biochemical explanation for the preferential mitofusin tethering reported in Mfn1 S329P and Mfn2 S350P expressing cells is that the proline is blocking conformational dynamics required for progression from mitofusin-tethered-mitochondria to lipid mixing and fusion of membranes. In the general context of membrane fusion, destabilization of membranes facilitates formation of a fusion pore and eventual lipid mixing. If the GTP-mediated conformational dynamics are required for formation of the fusion pore, and the conformational change during the transition state cannot occur, then this would block fusion. A study looking at the fusogenic capability of CMT2A-associated mitofusin variants revealed a role for cytosolic factors including but not limited to the apoptotic protein Bax in regulating mitochondrial fusion in cells, therefore it's possible that *agns-1* may be facilitating transition to lipid mixing in a mechanism that involves chaperone proteins. In the absence of GAPs or GEFs, a potential regulatory mechanism for mitofusin-mediated OMM fusion could be the stabilization of a conformational state to facilitate removal of the inorganic phosphate after hydrolysis, for example. Future work investigating additional cluster forming mitofusin variants will shed further light regarding whether the mechanism for the mitochondrial redistribution is consistent among all mitofusin variants.

### 2.3.1 Materials and Methods

*C elegans husbandry and maintenance*

Caenorhabditis strains were cultured on NGM plates seeded with OP50 E. coli, according to standard methods (Brenner, 1974).

*Molecular biology and transgenes*

A list of plasmids is provided in Supplement Table 1. Constructs were made using the three-slot multisite Gateway system from Invitrogen. The promoter sequence and coding sequence (cDNA), and C-terminal fluorescent markers were cloned along with a 3'UTR into the pCFJ90 destination vector. All insertions were made using direct injection, extrachromosomal arrays were integrated using UV irradiation.

*Cloning d2045.8*

*d2045.8* is the fourth gene in an operon that begins at the first gene, cul-3. Because of this, it is uncertain what promoter regulates expression of *d2045.8.* The coding sequence for *d2045.8* was cloned under the control of the EFT-3 and RAB-3 promoters, with a C-terminal GFP.

Isolation and identification of *d2045.8* mutation

*d2045.8 (um0017)* mutant was isolated from an EMS screen for suppressors of the uncoordinated locomotion associated with neuronal expression of murine Mfn1 S329P (*yakIS42*). When outcrossed away from two transgenic lines expressing murine Mfn1 S329P, *um0017* maintained a protruding vulval phenotype, defective locomotion and decreased progeny, the latter due at least in part to an increase in sterility.

The *um0017* mutation was mapped by following the phenotype, and crossing to alleles containing fluorescent markers on each of the six *C. elegans* chromosomes mapped *um0017* to a 6.1 Mb region on

Chromosome III. Whole genome sequencing of *um0017* in Mfn1 S329P expressing worms, as well as isolated *um0017*, identified eleven mutations consistent with EMS mutagenesis within the mapped region. Eight of the eleven were determined to be conserved in some manner across species, and within those two mutations were predicted to code for premature stop codons.

*Locomotion and egg-laying assays*

For locomotion and egg-laying assays, L4 worms were picked onto plates seeded with OP50 and allowed to mature overnight at room temperature.

To measure locomotion, first-day adults were picked onto thin lawns of OP50 and body bends were counted for one minute. A body bend was defined as the movement of a worm from minimum to maximum amplitude of the sine wave.

For egg laying assay, ten first-day adults were moved to fresh plates and allowed to lay eggs at room temperature. Eggs were counted every hour for a total period of four hours.

For proliferation and lifespan in early adulthood, 10 – 15 L4 were isolated onto individual plates seeded with OP50. Adults were moved onto new plates and number of eggs and larva were counted every day over the course of four days.

*Imaging and image analysis*

First-day adults were mounted onto 2% agarose pads and anesthetized using Levamisole. Images were obtained using a Nikon Ti-E wide-field microscope with a 60 x numerical aperture, 1.4 oil objective (Nikon), a solid-state light source (Spectra X, Lumencor), and an sCMOS camera (Zyla 5.5 megapixel). Each strain used was imaged on at least three occasions.

Images were analyzed using ImageJ software. Maximum intensity projections were created, and lines were drawn across the neuron overlapping with the fluorescent mitochondria. Fluorescent plot profiles measuring pixel intensity were then obtained for a trace covering approximately 100μM distance from the soma.

## 2.4 Figures

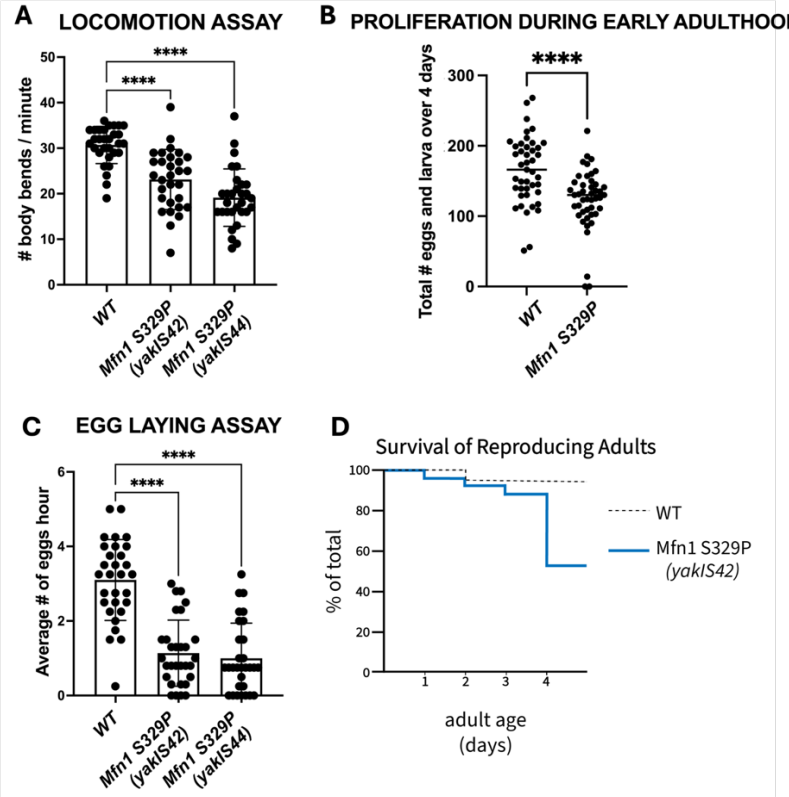


**Figure 2. 1 Expression of Mfn1 S329P in C elegans neurons produces phenotype associated with neuronal dysfunction.**

(A) D1 adult worms were picked onto a fresh plate seeded with OP50 and body bends were counted over a period of one minute. A full body bend is defined as the movement of a worm from max to min sine in the amplitude wave. n= 30 for all genotypes, 3 replicates of 10 worms.
(B, C) L4 worms were picked onto a fresh plate seeded with OP50 and were moved either every 24 hours for a period of 4 days (B) or every hour for a period of 4 hours (C). 3 replicates of 10 or more worms. Kruskal-Wallis test w/ Dunn's correction. Error bars = SEM. (D) percent of total animals plated and assayed over a period of four days. n>40 for all, over 3 replicates.

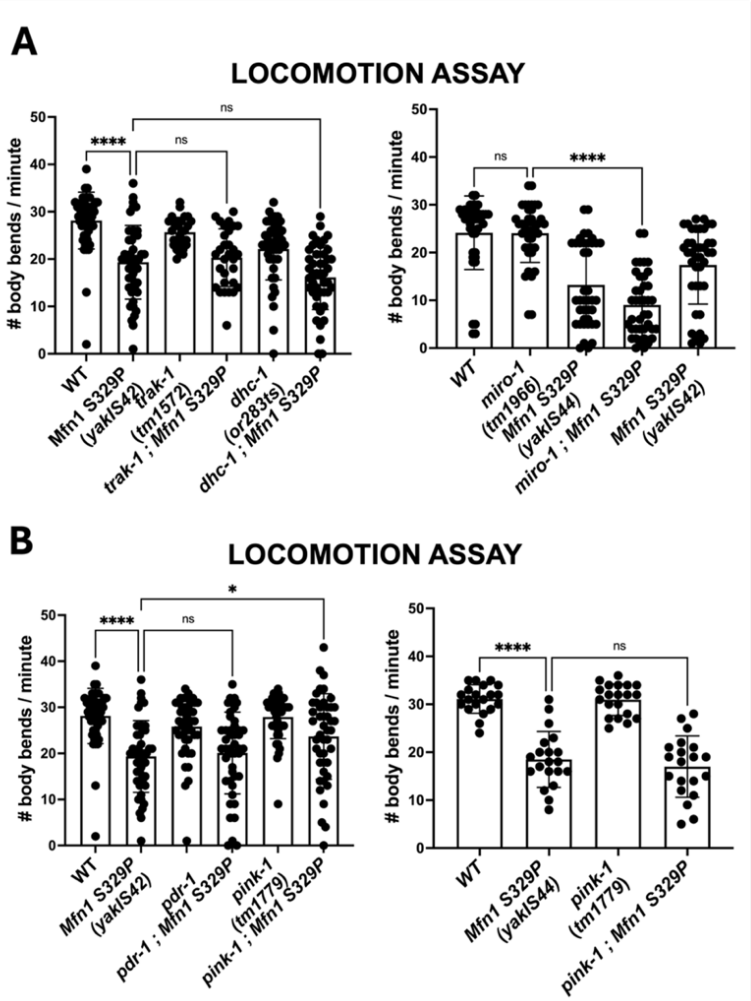


**Figure 2. 2 Candidate screen for suppressors of mutant Mfn1 S329P associated neuronal dysfunction.**

(A) Mutants of cytoskeletal transport adaptors miro-1 and trak-1 and retrograde motor dhc-1 assayed for suppression of uncoordinated locomotion (B) pink-1 and pdr-1 (Parkin) null mutants were crossed to mutant Mfn1 S329P transgenic worms and assayed for suppression of locomotion phenotype. n= 30, 3 replicates for all genotypes except Mfn1 S329P (yakIS44) and miro-1 (tm1966) single and double mutants, 2 replicates of 10 each. Kruskal-Wallis test w/ Dunn's correction. Error bars = SEM.

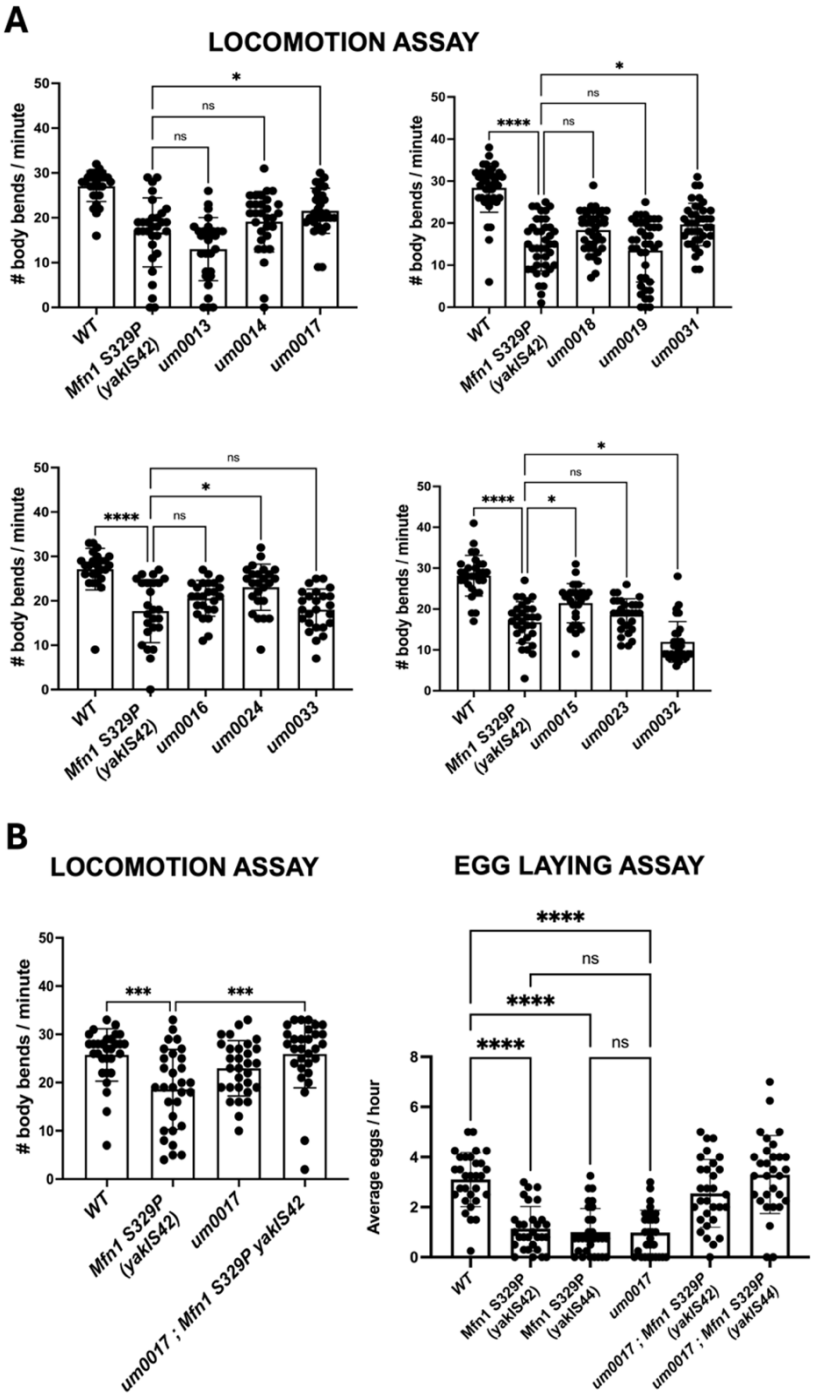


**Figure 2. 3 Candidate screen for suppressors of Mfn1 S329P associated neuronal dysfunction**

(A) F2 of EMS mutagenized worms were scored for suppression of mutant Mfn1 S329P transgene-associated uncoordinated locomotion. (B) *um0017* backcross tested for suppression of uncoordinated locomotion (left) and egg-laying defect (right). n = 30, 3 replicates of 10. Kruskal-Wallis test w/ Dunn's correction. Error bars = SEM.

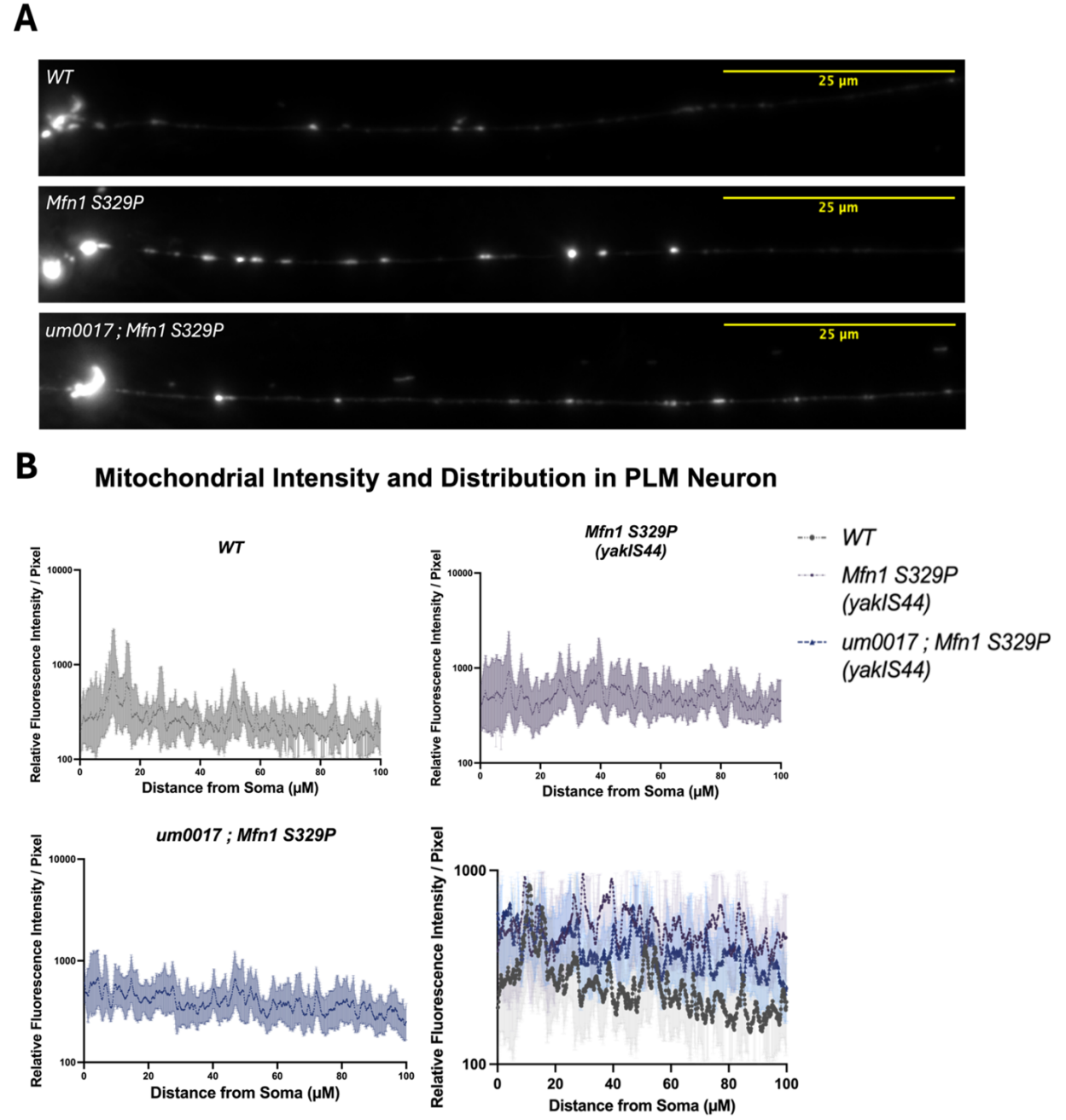


**Figure 2. 4 Mitochondria form clusters in touch neurons of Mfn1 S329P mutant worms**

A) Mitochondria in PLM neuron of WT, transgenic Mfn1 S329P, and mutant *um0017* ; Mfn1 S329P worms. Scale = 25µM. Left to right = soma to axon

B) Line trace profiles of mitochondria throughout 100µM of PLM neuron. Geometric mean and 95% Confidence Interval were plotted for WT, transgenic Mfn1 S329P, and double mutants *um0017* ; Mfn1 S329P worms.

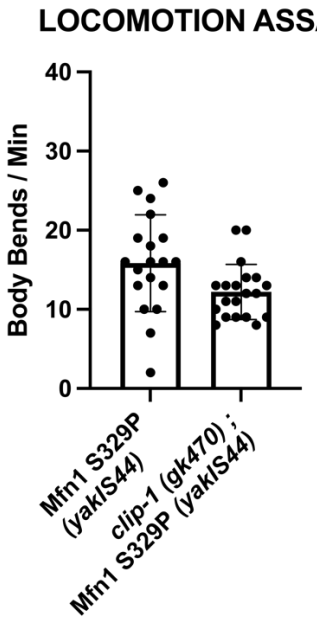


**Figure 2. 5 *clip-1 (gk470)* does not suppress neuronal phenotypes associated with expression of mutant Mfn1 S329P in worms.**

*n*= 20, 2 replicates of 10. Kruskal-Wallis test w/ Dunn's correction. Error bars = SEM.

## Table 1 Strains and Alleles

| GENE | CHR | STRAIN | ALLELE | FULL GENOTYPE |
|---|---|---|---|---|
| WT | | N2 Bristol | WT | |
| MFN1 | IV | XZ2257 | *yakIS42* | pRab3::MFN1S329P::Operon-GFP-NLS; pMyo2::mCherry |
| | | XZ2591 | *yakIS44* | |
| *dhc-1* (dynein) | I | EU1385 | *or283ts* | Temperature Sensitive embryonic lethal. 100% dead at 25° |
| *dhc-1* ; MFN1 | I ; IV | EU1385 ; XZ2257 | *or283ts ; yakIS42* | |
| *trak-1* | I | | *tm1572* | INSERTION: TTA (variant)<br>DELETION: 706bp deletion |
| *trak-1* ; MFN1 S329P | I ; IV | | *tm1572 ; yakIS42* | |
| *miro-1* | IV | | *tm1966* | INSERTION: ACC (variant)<br>DELETION: 408bp deletion |
| *miro-1 ;* MFN1 | IV ; ? | | *tm1966 ; yakIS44* | |
| *pdr-1* (parkin) | III | VC1024 | *gk448* | DELETION: 355 bp deletion |
| *pdr-1* ; MFN1 WT | III ; IV | VC1024 ; XZ2257 | *gk448 ; yakIS42* | |
| *pink-1 fbxl-1* | II | | *tm1779* | DELETION: 350bp deletion |
| *pink-1 fbxl-1 ;* MFN1 | II ; IV | | *tm1779 ; yakIS42* | |
| | | | *tm1779 ; yakIS44* | |
| *d2045.8* | III | VC20586 | *gk348738* | PREMATURE STOP: 501C<T |
| *d2045.8 ;* MFN1 | | VC20586 ; XZ2257 | *gk348738 ; yakIS42* | |
| | | | *gk348738 ; yakIS44* | |
| *d2045.8* | III | UM0017 | *um0017* | PREMATURE STOP: |
| *tomm-20* | | CLP215 | *twnEX8* | mec-7p::tom20::mChr ; myo2::GFP |
| | IV | UM0042 | *umIS1* | mec-7p::tom20::mChr ; myo2::GFP |
| *tomm-20 ;* MFN1 | IV ; ? | UM0042 ; XZ2591 | *umIS1 ; yakIS44* | mec-7p::tom20::mChr ; myo2::GFP ;<br>pRab3::MFN1S329P::Operon-GFP-NLS; pMyo2::mCherry |
| *tomm-20 ; d2045.8 ;* MFN1 | IV ; III ; ? | UM0042 ; UM0017 ; XZ2591 | *um0017 ; umIS1 ; yakIS44* | d2045.8 PREMATURE STOP ;<br>mec-7p::tom20::mChr ; myo2::GFP ;<br>pRab3::MFN1S329P::Operon-GFP-NLS; pMyo2::mCherry |
| | I-III | EG8040 | | oxTi302 I; oxTi75 II; oxTi411 unc-119(ed3) III; him-8(e1489) IV. |
| | IV-X | EG8041 | *oxTi76 ; oxTi405 ; oxTi421* | oxTi76 [eft-3p::GFP::H2B::tbb-2 3'UTR + unc-18(+)]; inserted in Chr. IV: 11,899,008. oxTi405 [eft-3p::tdTomato::H2B::unc-54 3'UTR + Cbr-unc-119(+)]; inserted in Chr. V: 15,838,568. oxTi421 [eft-3p::mCherry::tbb-2 3'UTR] inserted in Chr. X: 6,180,397. Him. |

# Chapter 3. Post-translational Regulation of Mitochondrial Dynamics

## 3.1 Introduction

Mitochondrial morphology and distribution can change in response to cellular needs to facilitate changes in mitochondrial function. Enzymes from the DSP family facilitate fission and fusion of mitochondria by mediating the remodeling of membranes. These opposing processes are tightly regulated, and the specific regulatory mechanisms have been a focus of interest due various reasons including the connections with disease. Disruptions in mitochondrial morphology have been reported in Alzheimer's Disease, Parkinson's Disease and Huntington's Disease models, among others, underscoring the significance of maintaining an adaptable mitochondrial network. A distinguishing feature of DSPs is that they do not require guanine nucleotide exchange factors (GEFs) or guanine nucleotide-activating proteins (GAPs). Thus, one way to regulate the activity of DSPs is through post-translational modifications. There is ample evidence for the regulation of mitochondrial morphology by targeting proteins associated with mitochondrial fission. Specifically, phosphorylation of Drp-1 S585 (rat) or S616 (humans) facilitates its association with adaptor proteins to increase mitochondrial fission during mitosis (Taguchi, Ishihara, Jofuku, Oka, & Mihara, 2007). During apoptosis, phosphorylation of Drp 1 S635 (rat) or S617 (humans) also promotes mitochondrial fragmentation (Cereghetti, Costa, & Scorrano, 2010; Cereghetti et al., 2008). Conversely, phosphorylation of Drp 1 S637 reduces GTPase activity, leading to a decrease in mitochondrial division (Chang & Blackstone, 2007). The post-translational regulation of Drp1 includes modifications beyond phosphorylation, such as S-nitrosylation and sumoylation (Cho et al., 2009; Figueroa-Romero et al., 2009). Phosphorylation of fission adaptor proteins such as MFF has also been reported to regulate mitochondrial morphology in response to cellular cues (Toyama et al., 2016).

The mitofusin paralogs, Mfn1 and Mfn2, are also regulated by post-translational modifications. Several kinases have been directly implicated in post-translational regulation of mitofusins. Specifically, PINK-1, ERK, PKA and JNK have been shown to phosphorylate either Mfn1 or Mfn2 in response to cellular stress, leading to inhibition of fusion to facilitate autophagy or cell death (Leboucher et al., 2012; Pyakurel, Savoia, Hess, & Scorrano, 2015a; Zhou et al., 2010). Mfn1 S228 was identified as a phosphorylation site in a large-scale analysis, and in the Hoppins Lab using mass spectrometry (MS)

(Leboucher et al., 2012; Lundby et al., 2013). This serine is conserved in Mfn2 and has been reported to be phosphorylated in one study, however, the implication of this phosphorylation event is unclear (Mendis, Rosenberg, & Azam, 2022).

Mfn1 S228/Mfn2 S249 S249 is in the highly conserved GTPase domain. The crystal structure of truncated Mfn1 bound to GDP depicts a mitofusin dimer in an open conformation, with alpha helices in the first helical bundle (HB1) pointing away from the globular GTPase domain (PDB 5GOM, Fig 3.1). Binding of the truncated Mfn1 to GDP BeF3, which mimics the transition state of GTP hydrolysis, leads to a rotation of the helical region relative to the GTPase domain, shifting the protein to a closed conformation (PDB 5YEW Fig 3.1). In the closed conformation, Mfn1 S228/Mfn2 S249 are within the region of the GTPase domain that is tightly opposed to HB1 (Cao et al., 2017). The closed conformation is stabilized by salt bridges formed between the GTPase domain and HB1 and these residues (D198 and D200) are near S228. In combination with reports of an associated CMT2A variant, Mfn2 S249F, this phosphorylation site became attractive due to its high potential for regulation by steric hindrance (Fig 3.1). The phosphate group would block the formation of the salt bridge, thereby disrupting conformational dynamics of the protein. Preliminary data characterizing the phosphomimetic variant Mfn1 S228E indicates that enzymatic activity is not affected, but fusion activity is deficient in vitro. Expression of the phosphomimetic variant in *MFN1* KO cells results in a redistribution of the mitochondrial network (Fig 3.2). Mfn1 S228E expression in cells does not result in degradation of the mitochondrial fusion complex, which has been reported for phosphorylation events on Mfn2 (Y. Chen & Dorn, 2013; Leboucher et al., 2012; Whitley, 2019). These data are consistent with a model where phosphorylation of Mfn1 S228 blocks fusion. To date, two phosphorylation sites in Mfn1 have been reported to modify its fusion ability, functioning to facilitate apoptosis. Unlike Mfn1 S228, Mfn1 T562 is within HB1, and the sequence around Mfn1 S228 does not resemble the canonical ERK site, which is the kinase reported to phosphorylate Mfn1 T562 (Pyakurel, Savoia, Hess, & Scorrano, 2015). Therefore, it's possible that a novel kinase and signaling pathway is responsible for the phosphorylation of Mfn1 S228. Here, the functional consequences of blocking phosphorylation at this site were further investigated. Although the biochemical data suggest mitochondrial fusion is blocked, it remains to be determined whether phosphorylation at

Mfn1 S228 occurs in response to a particular stress, or if it functions as a general regulatory mechanism for mitofusin-mediated OMM fusion.

## 3.2 Results

### 3.2.1 Cell Viability After Treatment with Apoptotic-Inducing Compounds

Biochemical data indicate that phosphorylation of Mfn1 S228 blocks mitochondrial fusion. Ongoing mitochondrial fission in conjunction with blocked mitochondrial fusion would lead to fragmentation of the mitochondrial network. This morphology is often associated with cellular stress responses and increased susceptibility to apoptosis (Lee et al., 2014; Toyama et al., 2016). For example, Mfn2 S27 is phosphorylated by JNK to trigger proteasomal degradation of mitofusins, which facilitates apoptosis by promoting a fragmented mitochondrial network (Leboucher et al., 2012). We hypothesized that this regulatory site on Mfn1 facilitates cell death by blocking mitochondrial fusion. We therefore predicted that blocking the phosphorylation by substitution of alanine at this site would prevent stress-induced mitochondrial fragmentation and cells expressing this variant would be less sensitive to cell death in response to stress. Because mitochondria are integrated into a variety of cellular stress pathways, we opted to screen several different stressors leading to cell death, focusing on compounds that target mitochondrial proteins or complexes. To quantify cell viability, we used the fluorescent reporter Calcein-AM, which becomes fluorescent when the AM group is cleaved by esterases within the cell. Cells were plated at equal densities and were treated overnight with stress-inducing compounds when nearly confluent. To obtain a reference readout of a population where nearly all cells are dead, the cells were fixed with methanol. The average change in fluorescence of cells treated with stress-inducing compounds was referenced to untreated controls of the same cell line to obtain a percent value of viable cells (Fig 3.3). Blocking translation using Puromycin resulted in variable differences in viability of Mfn1 WT cells compared to Mfn1 S228A phosphoblock cells over biological replicates, though no significant difference was observed in one pair of clonal populations reported. Cells treated with Antimycin A or Rotenone to inhibit ETC complexes I and III, respectively, did not exhibit significant differences in viability in Mfn1 WT vs Mfn1 phosphoblock cells.

Variability Variability among clonal populations expressing Mfn1 WT or Mfn1 S228A was observed, even when accounting for expression levels or cell density. Notably, the responses to Diamide, which alters cellular redox states, and Etoposide, which inhibits topoisomerase, were vastly different

among all cell lines assayed. Interestingly, treatment with Oligomycin to inhibit ATP synthase consistently resulted in decreased viability in cells expressing Mfn1 S228A across two single cell isolate populations.

### 3.2.2 Phenotypic analysis of cells expressing Mfn1 S228A

Mitochondrial morphology of clonal populations expressing Mfn1 S228A appears relatively unchanged when compared to the mitochondrial networks of cells expressing Mfn1 WT (Fig 3.4. When mitochondrial ATP production is compromised, cells can opt for alternative ways to produce energy, including increasing fatty acid oxidation (Zheng et al., 2023). Lipid droplets can be found throughout the cell, however they are associated with fatty acid oxidation when colocalizing with mitochondria. *MFN2* KO cells have reportedly fewer mitochondrial associated lipid droplets, therefore we posited that an accumulation of mitochondrial damage may result in an increase in lipid droplets to facilitate fatty acid oxidation. Fluorescence imaging of lipid droplets and mitochondria showed no significant change in lipid droplet localization or count in cells expressing Mfn1 WT or Mfn1 S228A in an *MFN1* KO background. To determine if there were any noticeable differences in cell size in response to metabolic disturbances, nuclear area was also compared between Mfn1 WT and Mfn1 S228A expressing cells. Again, no noticeable differences were observed among Mfn1 WT or Mfn1 S228A phosphoblock cells.

Fragmentation of the mitochondrial network is primarily associated with stress, but it has also been observed in mitotic cells (Rohn et al., 2014; Taguchi et al., 2007). Mitochondrial fragmentation during cell division ensures an even distribution and inheritance of mitochondria into daughter cells. This could result in slower cell growth or accumulation at a cell cycle check point therefore we assessed proliferation of Mfn1 WT and Mfn1 S228A cells over four days and no significant differences were observed (Table 2).

### 3.2.3 Coimmunoprecipitation of Mfn1-FLAG

Mfn2 S249, the serine equivalent to Mfn1 S228, was identified in a mass screen of the interactome of the MAPK pathway kinase TAK1. The specific physiological mechanism that activates TAK1 so that it targets mitofusin was not described (Mendis et al., 2022). TAK1 is implicated in various pathways that regulate cell death, including a proapoptotic MAP3K pathway (Fig 3.5A). Therefore, it is possible that TAK1, or another member of the MAPK pathway, may phosphorylate Mfn1 S228. p38 is a

proline directed kinase that is activated in response to stress conditions that lead to mitochondrial fragmentation (Canovas & Nebreda, 2021; Wada & Penninger, 2004). This kinase is a strong candidate because p38 has been shown to phosphorylate proteins in the OMM. In addition, the sequence recognition motif of p38 includes prolines near the phosphorylated serine, and Mfn1 S228 has a proline present near the serine. A physical interaction between TAK1 or p38 and mitofusin would be expected if either were phosphorylating Mfn1. To test this, a coimmunoprecipitation assay was performed using α-FLAG coated beads to enrich 3x-FLAG tagged Mfn1 WT expressed in Mfn1-null cells at near endogenous levels. As a negative control, α-GFP coated beads were used on equal samples and in parallel, while α-VDAC and α-tubulin were used. All samples were run under crosslinking or non-crosslinking conditions. p38 did not coelute with Mfn1-FLAG, though α-FLAG is not detectable, and all samples had detectable levels of tubulin. TAK1 eluted in the samples that were not cross-linked as well the negative α-GFP controls. Therefore, the results remain inconclusive.

### 3.3 Discussion

Our preliminary data demonstrate that a serine in the GTPase domain of Mfn1 can be phosphorylated and that this modifies mitofusin function (Fig 3.2). Previous reports of mitofusin phosphorylation have been in the context of the cellular stress response. For example, Mfn1 T562 has been reported to be phosphorylated by ERK to regulate apoptosis(Pyakurel et al., 2015). Therefore, we hypothesized that phosphorylation of Mfn1 S228 would occur in response to terminal cellular stress to facilitate apoptosis. Surprisingly, inhibition of ATP synthase by the compound Oligomycin consistently led to decreased viability in *MFN1* KO cells expressing the phosphoblock Mfn1 S228A in comparison with Mfn1 WT in all clonal populations reported (Fig 3.4). Interestingly, inhibition of ETC Complex III using Antimycin A did not result in significant differences in viability in Mfn1 phosphoblock vs Mfn1 WT cells. Oligomycin treatment can result in an accumulation of Reactive Oxygen Species (ROS), potentially causing mitochondrial stress. Stimulation of ROS formation by using the bacterial cell wall component LPS leads to activation of the nuclear transcription factor NFkB. In the absence of *MFN2*, cells are more susceptible to cell death following LPS-induced ROS activation suggesting MFN2 plays a protective role. This is supported by a decrease in autophagic flux in *MFN2* KO primary macrophages (Khodzhaeva et al., 2021). The MAPK p38 kinase is implicated in this response, linking this pathwkay once again to mitofusins. The western blot analysis and coimmunoprecipitation of the kinases p38 was inconclusive, therefore it should not be discarded as a putative kinase phosphorylating Mfn1.

In our experiments for viability, we observed vastly different responses to the oxidant Diamide between *MFN1* KO cells expressing Mfn1 S228A compared to Mfn1 WT and among clonal populations of cell lines stably expressing the same Mfn1 construct. Cells respond to stress in various ways, depending on the stressor and how much cellular functions are compromised. In response to short, localized stress or damage to mitochondria, cells can respond by attempting to repair the damage or remove the damaged organelle through mitophagy. However, when the requirement for correcting the damage is greater than the requirement for maintaining homeostasis, then stress response pathways can shift from corrective to apoptotic. Bax is a pro-apoptotic protein that has been reported to stimulate mitochondrial fusion in response to cellular stress (Du et al., 2021; Samanas et al., 2020). A marker for cell stress is the accumulation of Oxidized Glutathione (GSSG) which reacts with Cysteine in target proteins resulting in

generation of new disulfide bonds. Glutathione reductase (GR) catalyzes the conversion of GSSG to its reduced form (GSH) in an NADPH dependent manner. Increasing the concentration of intracellular GSSG by using the compound Diamide to oxidize GSH to GSSG was reported to cause an increase in mitochondrial hyperfusion in cells, reportedly due to a requirement of Mfn2 C684 for fusion. It was also reported that stress-induced mitochondrial hyperfusion may require ROS (Shutt, Geoffrion, Milne, & McBride, 2012). Thus, the full impact of redox state on Mfn1 S228 phosphorylation could not be determined based on the results from the viability experiment.

The results obtained from the viability experiment, together with the lack of an obvious phenotype in MEF cells could neither support nor deny the hypothesis posited. It is possible that Mfn2 or other pathways may be active to compensate for loss of Mfn1 S228, however the mechanisms remain to be determined.

## 3.4 Materials and Methods

*Generation of stable cell lines*

MEF *MFN1* WT and *MFN1* KO cells were obtained from ACTT. Cells expressing Mfn1 S228 phosphomimetic and phosphovariant were screened for Mfn1 expression at near endogenous levels, and at least two different clonal populations of each cell line were consistently used. Data acquisition was performed blind when appropriate and feasible.

*Cell Viability Assay*

Cells were seeded onto ~1500 per well in a 96-well black microplates treated with polystyrene (Falcon BD353376) in DMEM + GlutaMax. After 22 – 24 hours, cells were incubated with compounds to induce a stress response for 16-18 hours. After incubation, cells were washed two times with PBS warmed to 37° to remove esterases present in the culture media, and then 100nM Calcein AM (Invitrogen) in PBS was added to wells. Fluorescence values at 515nm were obtained every 15 minutes for at least one hour. The change in fluorescence between each timepoint relates to the amount of estherases present in living cells able to cleave off the AM group. To obtain percent viability, the average change in fluorescence at 515nm was obtained for treated cells as a measure of enzyme activity, and referenced to the average change in fluorescence of untreated cells from the same single cell isolate population. At least three individual replicates of six wells are reported. n>20 for all.

*Coimmunoprecipitation of Mfn1-FLAG*

Cells were permeabilized with IPLB Complete (20mM HEPES-KOH pH 7.4, 150mM KOAc, 2mM Mg $(AC)_2$, 1mM EGTA, 0.6M Sorbitol plus 1% w/v Digitonin and PMSF prior to BCA assay to measure protein concentration.

For coimmunoprecipitation of Mfn1-FLAG, 50µL uMACS beads were added to 1mg of total cell lysate and incubated with rotation for at least 1 hour. Columns were equilibrated using IPLB complete prior to adding samples. Columns were washed twice in wash buffer (20mM HEPES-KOH pH8, 150mM KOAc, 2mM

Mg(Ac)2, 1mM EGTA and 0.6M Sorbitol) containing PMSF, and washed a third time in wash buffer without KOAc, PMSF or Digitonin. Samples were then eluted in 2X Laemlli buffer heated to 95°.

For coimmunoprecipitation of Mfn1-FLAG, 50µL uMACS beads were added to 1mg of total cell lysate and incubated with rotation for at least 1 hour. Columns were equilibrated using IPLB complete prior to adding samples. Columns were washed 3 times, then incubated with warm Laemlli buffer prior to elution.

### 3.5 Figures

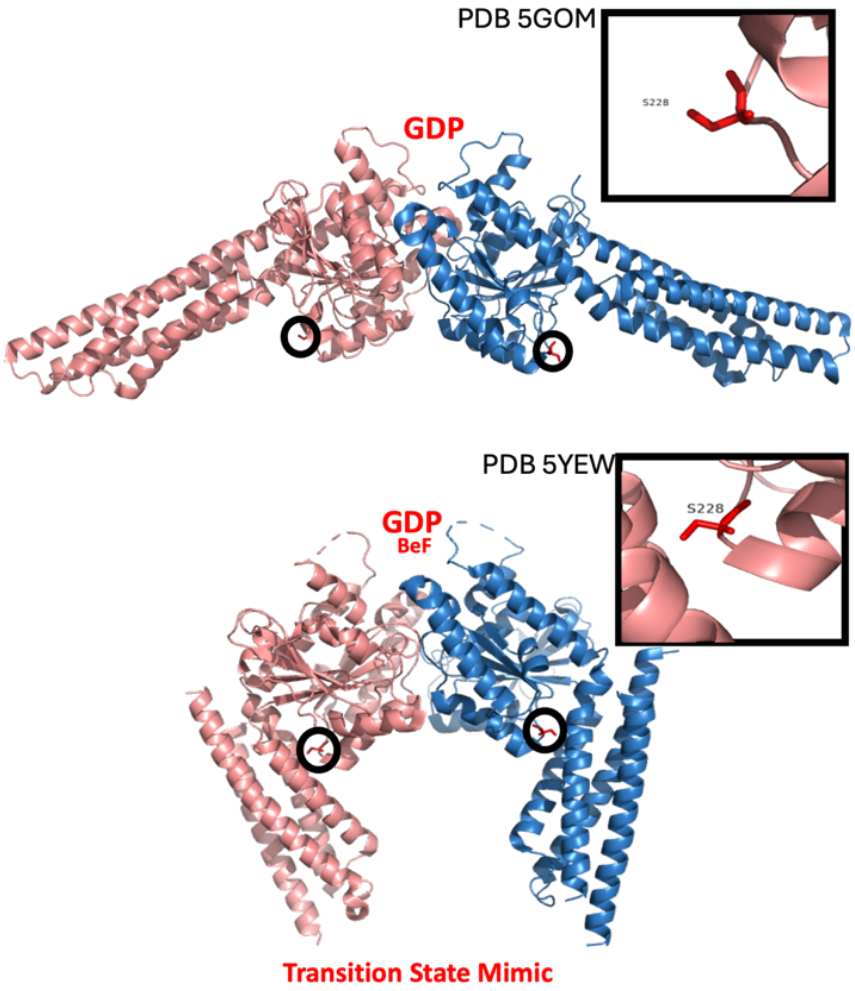


**Figure 3. 1 Mfn1 is Phosphorylated at S228**

Crystal structure of Mfn1 GTPase domain and HB1. Structure on the top was obtained in presence of GDP (PDB 5GOM). This intermolecular interface between globular GTPase domains activates GTP hydrolysis in the dynamin family. Structure on the bottom was obtained using a transition state mimic, GDP $BeF_3$ (PDB 5YEW). A conformational change was observed in comparing the GDP bound and the transition state mimic, where the helical bundles have moved relative to the GTPase domain. Mfn1 S228 is highlighted in both conformations with residue zoomed in. Equivalent serine in Mfn2 is S249. Mfn2 S249F associated with disease.

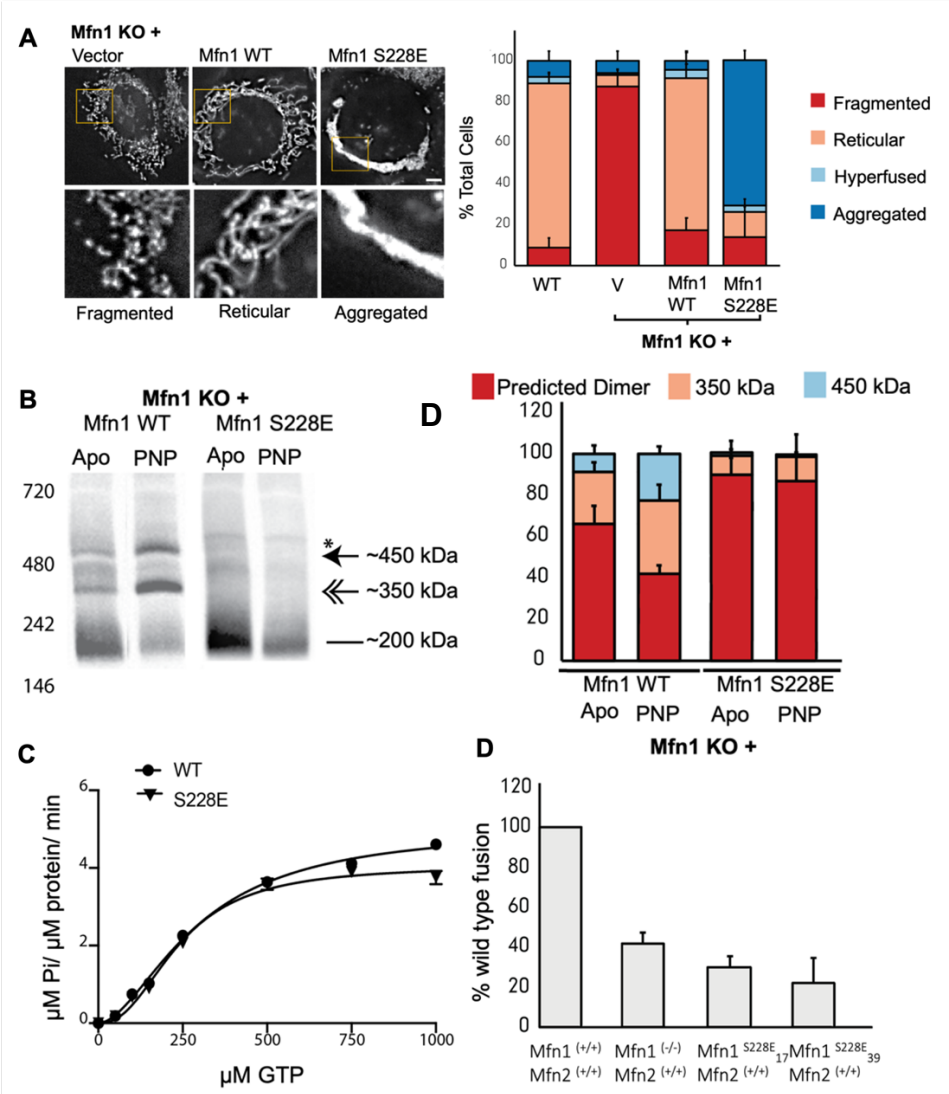


**Figure 3. 2 Biochemical Analysis of Mfn1 S228E**

(A) Representative images of *MFN1* KO MEFs transduced with either empty vector, WT Mfn1 or the phosphorylation mimic Mfn1 S228E. Mitochondrial morphology was scored based on size and distribution of mitochondria. Quantification represents blinded counts from at least 100 cells in three independent experiments (error = SD). Scale bar is 5μM. (B) BN-PAGE of full length, native Mfn1 from isolated mitochondria. Mitochondria were isolated from clonal populations of *MFN1* KO MEF cells expressing Mfn1 WT or Mfn1 S228E. Untreated mitochondria were incubated for 30 minutes while treated mitochondria were incubated with the specific nucleotide at 30°C for 30 minutes. Mitochondria were then lysed, subjected to BN-PAGE, and immunoblotted with an anti-FLAG antibody. Asterisk indicates a non-specific band from the anti-FLAG antibody. Protein complexes are indicated with lines/arrows as either a predicted dimer (straight line), ~320kD (double arrowhead) and ~450kDa (arrowhead). (B) The distribution of protein is indicated in the bar graph as a mean + SD of two independent experiments. (C) Kinetic analysis of GTP hydrolysis in wild-type Mfn1 minimal GTPase domain (MGD) and Mfn1 S228E MGD. (D) Mitochondria were isolated from wild-type cells, from a clonal population of *MFN1* KO cells transduced with an empty vector ($Mfn1^{-/-}$ $Mfn^{2+/+}$), and two clonal populations of *MFN1* KO transduced with Mfn1 S228E to determine fusion. ***Adapted from Whitley Dissertation.**

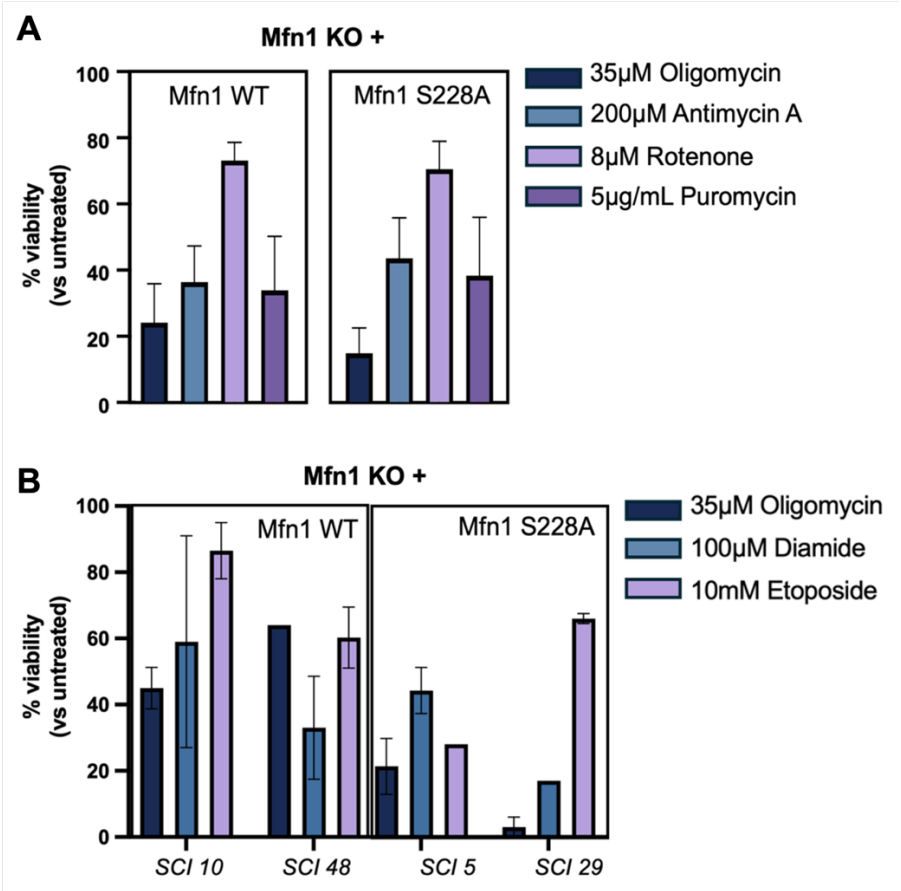


**Figure 3. 3 Cell viability of Mfn1 KO MEF cells transduced with Mfn1 WT.**
Cells are seeded onto 96-well dishes and incubated with corresponding compounds to induce a stress response for 16-18 hours. Cells are then washed with PBS and incubated Calcein-AM, which binds specifically to live cells. Fluorescence at 520nm is measured using a plate reader every 15 minutes over a period of one hour. Reported values are average change in fluorescence per 15 minutes in treated vs untreated of the same single cell isolate clonal population (SCI). (A) represents Mfn1 KO + Mfn1 WT, SCI 10 and Mfn1 S228A, SCI 5. (B) Two pairs of individual SCI were assessed for Mfn1 KO + WT and Mfn1 KO + S228A.

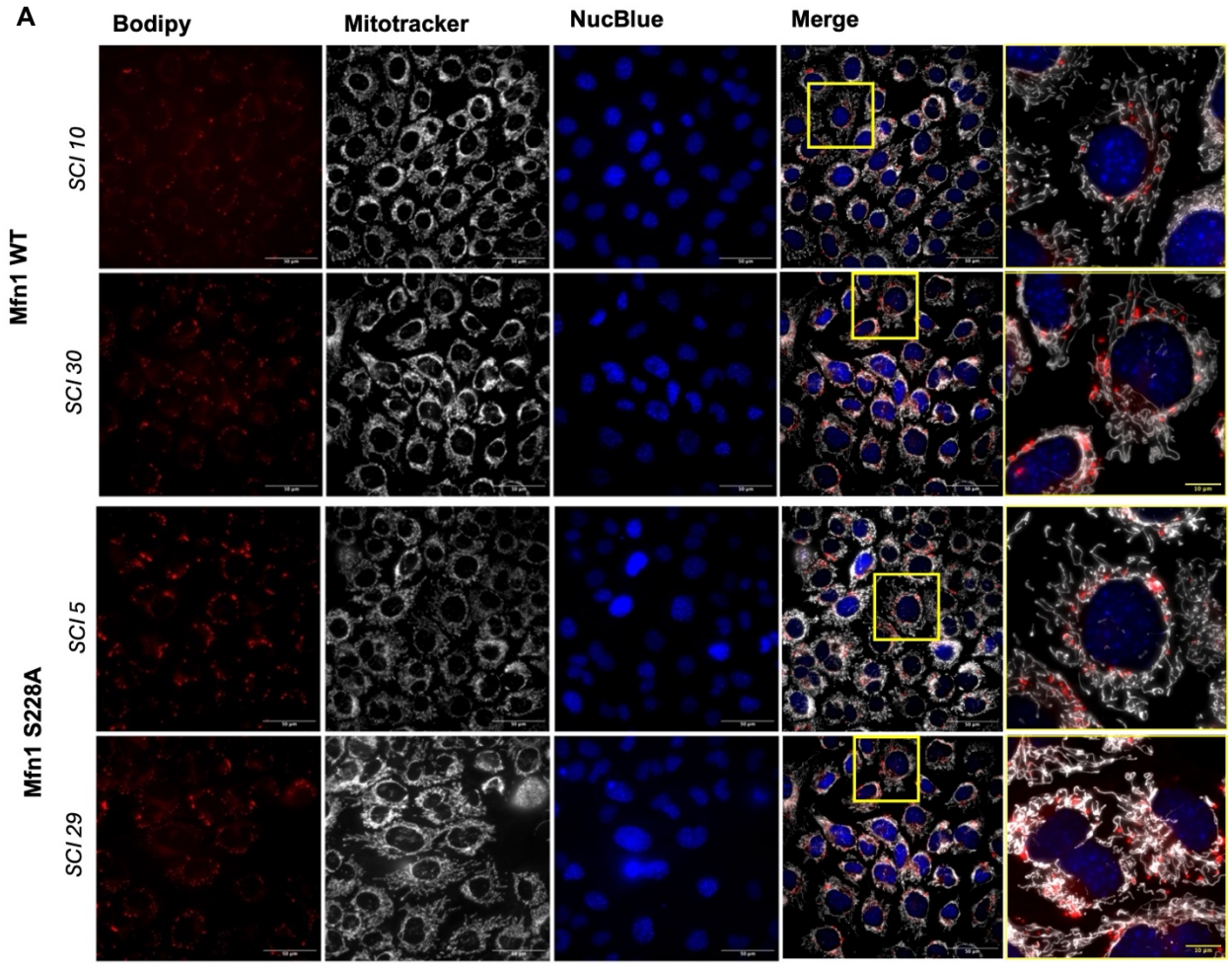
A
Bodipy
Mitotracker
NucBlue
Merge
Mfn1 WT
SCI 10
SCI 30
Mfn1 S228A
SCI 5
SCI 29

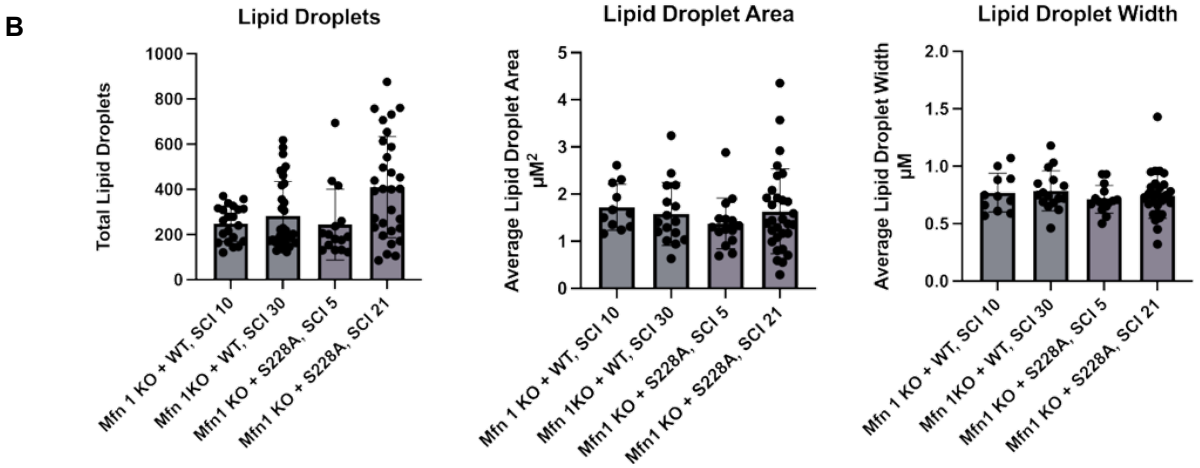
B
Lipid Droplets
Total Lipid Droplets
1000
800
600
400
200
0
Mfn 1 KO + WT, SCI 10
Mfn 1KO + WT, SCI 30
Mfn1 KO + S228A, SCI 5
Mfn1 KO + S228A, SCI 21
Lipid Droplet Area
Average Lipid Droplet Area µM2
5
4
3
2
1
0
Lipid Droplet Width
Average Lipid Droplet Width µM
2.0
1.5
1.0
0.5
0.0

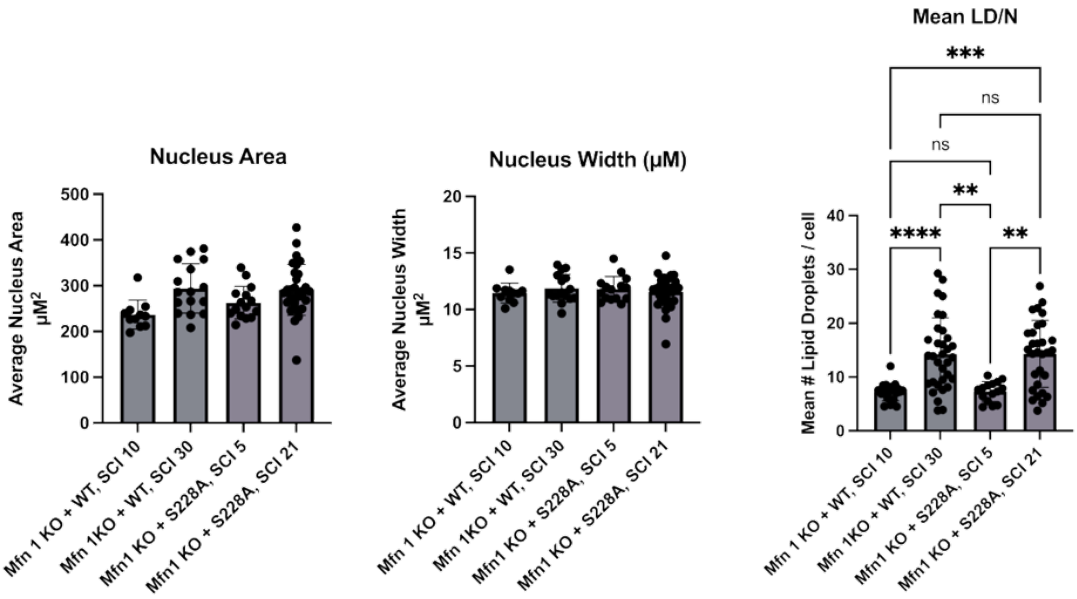


**Figure 3. 4 No Significant Phenotypic Differences in Mfn1 S228A vs Mfn1 WT**

(A) MEF Mfn1 KO + Mfn1 WT, or Mfn1 KO + Mfn1 S228A were grown to confluency and prior to imaging treated with Bodipy to visualize lipid droplets, mitochtracker and NucBlue. Blinded experiments scored differences in (B) Lipid Droplets and nuclei in triplicate with at least 100 cells.

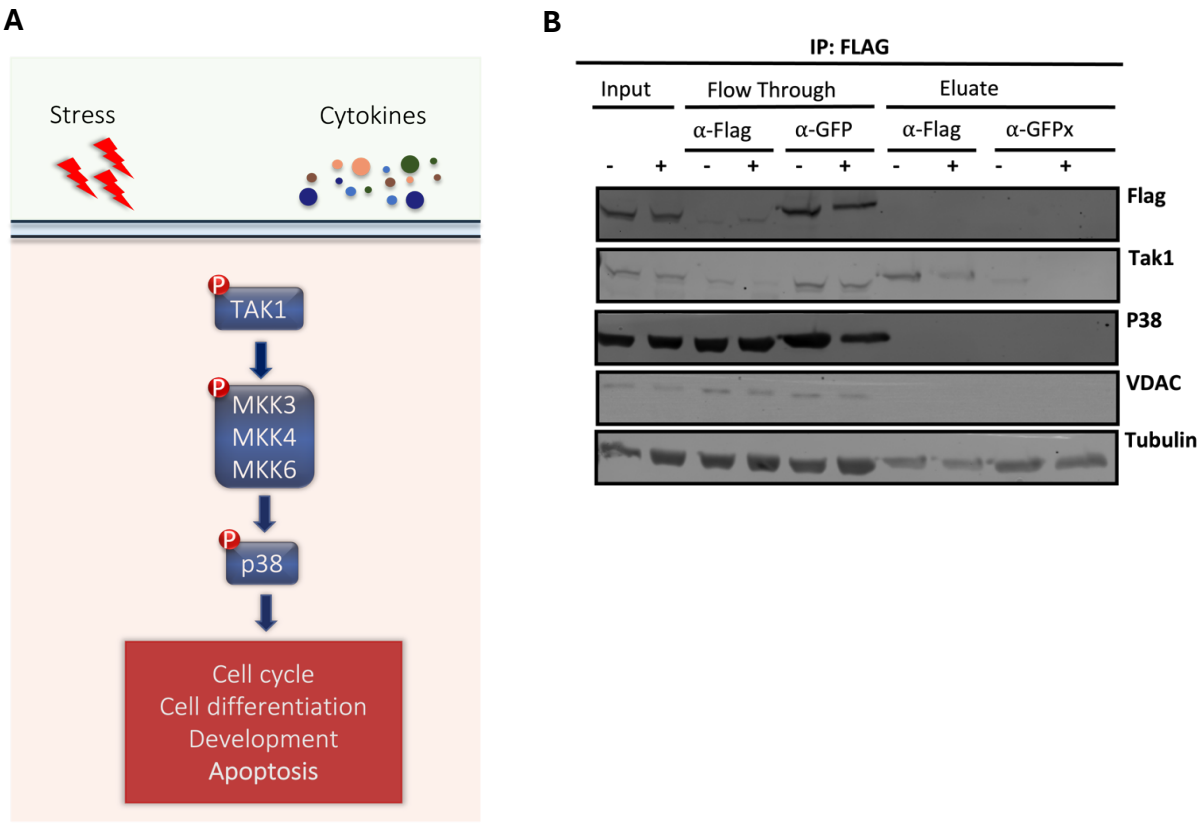


**Figure 3. 5 Kinases from MAPK pathway may phosphorylate Mfn1 S228**

(A) Extracellular cues such as cytokines or stress activate kinases that phosphorylate TAK1. Activated TAK1 then phosphorylates MKK3, MKK4 or MKK6, which subsequentially phosphorylate p38. p38 phosphorylation activates transcription factors involved in several cellular pathways, including apoptosis. (B) Western Blot of Mfn1 S329P-3X FLAG isolated using α-FLAG coated beads, then probed for a physical interaction with TAK1 or p38.

**Table 2 Cell Proliferation of Clonal Populations**

| Cell Line | Total Cells after 4 days | % Viable (out of total) |
|---|---|---|
| MFN1 KO + MFN1 WT, SCI 10 | 1.1 x 106 | 97% |
| MFN1 KO + MFN1 WT, SCI 30 | 6.5 x 105 | 92% |
| MFN1 KO + MFN1 S228A, SCI 10 | 1.8 x 106 | 96% |
| MFN1 KO + MFN1 S228A, SCI 29 | 4.1 x 105 | 95% |

# Chapter 4. Conclusions and Future Directions

## 4.1 Summary of mutant Mfn1 genetic screen in *C. elegans*

### 4.1.1 Bridging the gap between in vitro and in vivo

In this study, we expressed the biochemically characterized murine mitofusin variant Mfn1 S329P in *C. elegans* and report locomotor defects consistent with neuronal dysfunction. We performed genetic screens for suppressors of the locomotion phenotype associated with expression of Mfn1 S329P and have identified a novel gene, agns-1, as facilitator of mitochondrial aggregation. Of significant interest is the finding that Mfn1 S329P associated mitochondrial clusters exist throughout the axon of the neuron, and not exclusively in the soma. Aggregates are a hallmark of many neurodegenerative diseases, including Alzheimer's Disease. One model for neurodegeneration in tauopathies or other aggregate accumulating diseases posits that exposure to the protein surface of hydrophobic residues that are typically buried within the protein core can lead to accumulation of proteins that cannot be easily degraded. Mutations in which protein misfolding leads to exposure of typically buried hydrophobic residues to the protein surface have been suggested to be a possible mechanism behind the formation of aggregates in various neurodegenerative diseases. The appearance of more intense and larger puncta in the neurons of Mfn1 S329P transgenic worms could suggest an increase in mitochondrial content, decreased turnover of mitochondrial proteins, or accumulation of peptides due to exposed sticky residues. These possibilities are not mutually exclusive and, given the numerous reports of aggregate formation in neurons leading to or exacerbating neurodegeneration, warrant further investigation. It is noteworthy that mitochondrial clusters were observed across distances greater than 100μM, however it is unclear whether neurodegeneration was also present because neuronal lengths were not scored in conjunction with mitochondrial clusters. Further experiments to dissect the composition of clusters and the relationship to neuronal morphology will clarify whether the neuronal dysfunction is caused by neuronal degeneration, or a consequence of impeding synaptic function.

### 4.1.2 Roles for actin in facilitating or disrupting mitofusin function

*agns-1* homologs are reported to function in various pathways where Rho A is a downstream target. Rho A and other actin binding and actin nucleating proteins are associated with mitochondrial transport and Drp-1. Thus, the link to actin should be further explored. Depolymerization of actin in cells expressing CMT2A-associated variants that have been biochemically characterized in terms of enzyme activity and fusogenic function will further determine the contributions of actin to mitochondrial fusion.

### 4.2 Phosphorylation of Mfn1 S228

One possible explanation for the variability observed in the viability experiments could be Mfn2 activity in the background, in combination with additional factors compensating for loss of phosphorylation at Mfn1 S228. To account for this, the same experiments can be performed in an MFN1 KO + MFN1 WT background where Mfn2 expression is decreased. Given the variability observed in clonal populations of MFN1 KO cells expressing either Mfn1 WT or Mfn1 S228A, a large-scale omics analysis may yield more insight. For instance, RNA seq can inform whether there are significant differences in expression levels of stress response pathways that are consistent among clonal populations of Mfn1 S228A. Finally, the sensitivity of cells expressing Mfn1 S228A to Oligomycin-induced cell death should be further explored. I predict that ROS signaling for survival may be disrupted if mitochondrial function is compromised. Therefore, I suggest looking further into mitochondrial respiratory capacity in cells expressing phosphoblock Mfn1 S228A.

## Chapter 5. Supplementary Figures

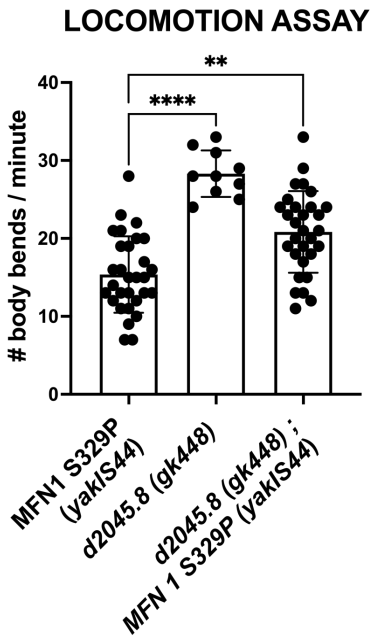


**Figure S 1 *d2045.8 (gk348738)* Heterozygotes Suppress Uncoordinated Locomotion in Transgenic Worms Expressing Mfn1 S329P.** Confirmed by sequencing to be heterozygotes.

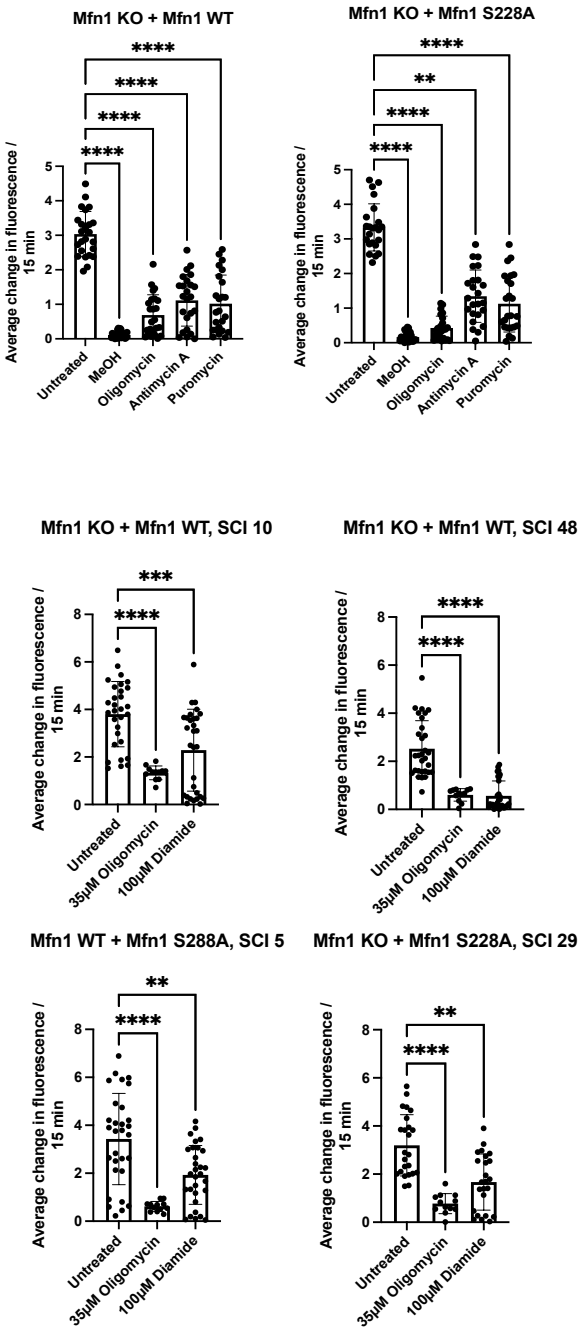


**Figure S 2 Treatment with stress-inducing compounds triggers cell death**

## Chapter 6. References


Ahn, S. Y., Li, C., Zhang, X., & Hyun, Y. M. (2018). Mitofusin-2 expression is implicated in cervical cancer pathogenesis. *Anticancer Research*, *38*(6), 3419–3426. https://doi.org/10.21873/anticanres.12610

Angajala, A., Lim, S., Phillips, J. B., Kim, J. H., Yates, C., You, Z., & Tan, M. (2018). Diverse roles of mitochondria in immune responses: Novel insights into immuno-metabolism. *Frontiers in Immunology*, *9*(JUL). https://doi.org/10.3389/fimmu.2018.01605

Babic, M., Russo, G. J., Wellington, A. J., Sangston, R. M., Gonzalez, M., & Zinsmaier, K. E. (2015). Miro's N-terminal GTPase domain is required for transport of mitochondria into axons and dendrites. *The Journal of Neuroscience : The Official Journal of the Society for Neuroscience*, *35*(14), 5754–5771. https://doi.org/10.1523/JNEUROSCI.1035-14.2015

Baloh, R. H., Schmidt, R. E., Pestronk, A., & Milbrandt, J. (2007). Altered axonal mitochondrial transport in the pathogenesis of Charcot-Marie-Tooth disease from mitofusin 2 mutations. *Journal of Neuroscience*, *27*(2), 422–430. https://doi.org/10.1523/JNEUROSCI.4798-06.2007

Bocanegra, J. L., Adikes, R., & Quintero, O. A. (2020). Myosin XIX. *Advances in Experimental Medicine and Biology*, *1239*, 439–451. https://doi.org/10.1007/978-3-030-38062-5_20

Bocanegra, J. L., Fujita, B. M., Melton, N. R., Cowan, J. M., Schinski, E. L., Tamir, T. Y., … Quintero, O. A. (2019). The MyMOMA domain of MYO19 encodes for distinct Miro-dependent and Miro-independent mechanisms of interaction with mitochondrial membranes. *Cytoskeleton*, (August), 1–18. https://doi.org/10.1002/cm.21560

Boldogh, I. R., & Pon, L. A. (2006). Interactions of mitochondria with the actin cytoskeleton. *Biochimica et Biophysica Acta (BBA) - Molecular Cell Research*, *1763*(5), 450–462. https://doi.org/https://doi.org/10.1016/j.bbamcr.2006.02.014

Brenner, S. (1974). THE GENETICS OF CAENORHABDITIS ELEGANS. *Genetics*, *77*(1), 71–94. https://doi.org/10.1093/genetics/77.1.71

Brickley, K., & Stephenson, F. A. (2011). Trafficking Kinesin Protein (TRAK)-mediated Transport of Mitochondria in Axons of Hippocampal Neurons. *Journal of Biological Chemistry* , *286*(20), 18079–18092. https://doi.org/10.1074/jbc.M111.236018

Byrne, J. J., Soh, M. S., Chandhok, G., Vijayaraghavan, T., Teoh, J. S., Crawford, S., … Neumann, B. (2019). Disruption of mitochondrial dynamics affects behaviour and lifespan in Caenorhabditis elegans. *Cellular and Molecular Life Sciences*, *76*(10), 1967–1985. https://doi.org/10.1007/s00018-019-03024-5

Canovas, B., & Nebreda, A. R. (2021). Diversity and versatility of p38 kinase signalling in health and disease. *Nature Reviews Molecular Cell Biology*, *22*(5), 346–366. https://doi.org/10.1038/s41580-020-00322-w

Cao, Y. L., Meng, S., Chen, Y., Feng, J. X., Gu, D. D., Yu, B., … Gao, S. (2017). MFN1 structures reveal nucleotide-triggered dimerization critical for mitochondrial fusion. *Nature*, *542*(7641), 372–376.

https://doi.org/10.1038/nature21077

Cereghetti, G. M., Costa, V., & Scorrano, L. (2010). Inhibition of Drp1-dependent mitochondrial fragmentation and apoptosis by a polypeptide antagonist of calcineurin. *Cell Death and Differentiation*, *17*(11), 1785–1794. https://doi.org/10.1038/cdd.2010.61

Cereghetti, G. M., Stangherlin, A., Martins De Brito, O., Chang, C. R., Blackstone, C., Bernardi, P., & Scorrano, L. (2008). Dephosphorylation by calcineurin regulates translocation of Drp1 to mitochondria. *Proceedings of the National Academy of Sciences of the United States of America*, *105*(41), 15803–15808. https://doi.org/10.1073/pnas.0808249105

Chada, S. R., & Hollenbeck, P. J. (2003). Mitochondrial movement and positioning in axons: The role of growth factor signaling. *Journal of Experimental Biology*, *206*(12), 1985–1992. https://doi.org/10.1242/jeb.00263

Chan, D. C. (2020). Mitochondrial Dynamics and Its Involvement in Disease. *Annual Review of Pathology: Mechanisms of Disease*, *15*, 235–259. https://doi.org/10.1146/annurev-pathmechdis-012419-032711

Chang, C. R., & Blackstone, C. (2007). Cyclic AMP-dependent protein kinase phosphorylation of Drp1 regulates its GTPase activity and mitochondrial morphology. *Journal of Biological Chemistry*, *282*(30), 21583–21587. https://doi.org/10.1074/jbc.C700083200

Chen, H., Detmer, S. A., Ewald, A. J., Griffin, E. E., Fraser, S. E., & Chan, D. C. (2003). Mitofusins Mfn1 and Mfn2 coordinately regulate mitochondrial fusion and are essential for embryonic development. *Journal of Cell Biology*, *160*(2), 189–200. https://doi.org/10.1083/jcb.200211046

Chen, Y., & Dorn, G. W. (2013). PINK1-Phosphorylated Mitofusin 2 Is a Parkin Receptor for Culling Damaged Mitochondria. *Science*, *340*(6131), 471–475. https://doi.org/10.1126/science.1231031

Chen, Y., Liu, Y., & Dorn, G. W. (2011). Mitochondrial fusion is essential for organelle function and cardiac homeostasis. *Circulation Research*, *109*(12), 1327–1331. https://doi.org/10.1161/CIRCRESAHA.111.258723

Cho, D.-H., Nakamura, T., Fang, J., Cieplak, P., Godzik, A., Gu, Z., & Lipton, S. A. (2009). S-Nitrosylation of Drp1 Mediates β-Amyloid-Related Mitochondrial Fission and Neuronal Injury. *Science*, *324*(5923), 102–105. https://doi.org/10.1126/science.1171091

Dai, W., & Jiang, L. (2019). Dysregulated Mitochondrial Dynamics and Metabolism in Obesity, Diabetes, and Cancer. *Frontiers in Endocrinology*, *10*(September), 1–10. https://doi.org/10.3389/fendo.2019.00570

Davis, K., Basu, H., Izquierdo-Villalba, I., Shurberg, E., & Schwarz, T. L. (2023). Miro GTPase domains regulate the assembly of the mitochondrial motor-adaptor complex. *Life Science Alliance*, *6*(1), 1–21. https://doi.org/10.26508/lsa.202201406

Davis, P., Zarowiecki, M., Arnaboldi, V., Becerra, A., Cain, S., Chan, J., … Sternberg, P. W. (2022). WormBase in 2022-data, processes, and tools for analyzing Caenorhabditis elegans. *Genetics*, *220*(4). https://doi.org/10.1093/genetics/iyac003

Detmer, S. A., & Chan, D. C. (2007). Complementation between mouse Mfn1 and Mfn2 protects mitochondrial fusion defects caused by CMT2A disease mutations. *Journal of Cell Biology*, *176*(4), 405–414. https://doi.org/10.1083/jcb.200611080

Dorn, G. W. (2020). Mitofusins as mitochondrial anchors and tethers. *Journal of Molecular and Cellular Cardiology*, *142*(January), 146–153. https://doi.org/10.1016/j.yjmcc.2020.04.016

Du, M., Yu, S., Su, W., Zhao, M., Yang, F., Liu, Y., … Chen, T. (2021). Mitofusin 2 but not mitofusin 1 mediates Bcl-XL-induced mitochondrial aggregation. *Journal of Cell Science*, *133*(20). https://doi.org/10.1242/jcs.245001

El Fissi, N., Rojo, M., Aouane, A., Karatas, E., Poliacikova, G., David, C., … Rival, T. (2018). Mitofusin gain and loss of function drive pathogenesis in Drosophila models of CMT 2A neuropathy . *EMBO Reports*, *19*(8), 1–16. https://doi.org/10.15252/embr.201745241

Feely, S. M. E., Laura, M., Siskind, C. E., Sottile, S., Davis, M., Gibbons, V. S., … Shy, M. E. (2011). MFN2 mutations cause severe phenotypes in most patients with CMT2A. *Neurology*, *76*(20), 1690–1696. https://doi.org/10.1212/WNL.0b013e31821a441e

Fenton, A. R., Jongens, T. A., & Holzbaur, E. L. F. (2021). Mitochondrial adaptor TRAK2 activates and functionally links opposing kinesin and dynein motors. *Nature Communications*, *12*(1), 1–15. https://doi.org/10.1038/s41467-021-24862-7

Figueroa-Romero, C., Iñiguez-Lluhí, J. A., Stadler, J., Chang, C.-R., Arnoult, D., Keller, P. J., … Feldman, E. L. (2009). SUMOylation of the mitochondrial fission protein Drp1 occurs at multiple nonconsensus sites within the B domain and is linked to its activity cycle. *FASEB Journal : Official Publication of the Federation of American Societies for Experimental Biology*, *23*(11), 3917–3927. https://doi.org/10.1096/fj.09-136630

Filadi, R., Pendin, Di., & Pizzo, P. (2018). Mitofusin 2: From functions to disease. *Cell Death and Disease*, *9*(3). https://doi.org/10.1038/s41419-017-0023-6

Fransson, Å., Ruusala, A., & Aspenström, P. (2003). Atypical Rho GTPases have roles in mitochondrial homeostasis and apoptosis. *Journal of Biological Chemistry*, Vol. 278, pp. 6495–6502. https://doi.org/10.1074/jbc.M208609200

Fransson, Å., Ruusala, A., & Aspenström, P. (2006). The atypical Rho GTPases Miro-1 and Miro-2 have essential roles in mitochondrial trafficking. *Biochemical and Biophysical Research Communications*, *344*(2), 500–510. https://doi.org/10.1016/j.bbrc.2006.03.163

Gatti, P., Schiavon, C., Cicero, J., Manor, U., & Germain, M. (2024). Mitochondria- and ER-associated actin are required for mitochondrial fusion. *Nature Communications*, (August 2024). https://doi.org/10.1101/2023.06.13.544768

Ge, Y., Shi, X., Boopathy, S., McDonald, J., Smith, A. W., & Chao, L. H. (2020). Two forms of opa1 cooperate to complete fusion of the mitochondrial inner-membrane. *ELife*, *9*, 1–22. https://doi.org/10.7554/eLife.50973

Glater, E. E., Megeath, L. J., Stowers, R. S., & Schwarz, T. L. (2006). Axonal transport of mitochondria

requires milton to recruit kinesin heavy chain and is light chain independent. *Journal of Cell Biology*, *173*(4), 545–557. https://doi.org/10.1083/jcb.200601067

Guo, X., Macleod, G. T., Wellington, A., Hu, F., Panchumarthi, S., Schoenfield, M., … Zinsmaier, K. E. (2005). The GTPase dMiro is required for axonal transport of mitochondria to drosophila synapses. *Neuron*, *47*(3), 379–393. https://doi.org/10.1016/j.neuron.2005.06.027

Hales, K. G., & Fuller, M. T. (1997). Developmentally regulated mitochondrial fusion mediated by a conserved, novel, predicted GTPase. *Cell*, *90*(1), 121–129. https://doi.org/10.1016/S0092-8674(00)80319-0

Hawthorne, J. L., Mehta, P. R., Singh, P. P., Wong, N. Q., & Quintero, O. A. (2016). Positively charged residues within the MYO19 MyMOMA domain are essential for proper localization of MYO19 to the mitochondrial outer membrane. *Cytoskeleton (Hoboken, N.J.)*, *73*(6), 286–299. https://doi.org/10.1002/cm.21305

Hollenbeck, P. J., & Saxton, W. M. (2005). The axonal transport of mitochondria. *Journal of Cell Science*, *118*(Pt 23), 5411–5419. https://doi.org/10.1242/jcs.02745

Hoseini, H., Pandey, S., Jores, T., Schmitt, A., Franz-Wachtel, M., Macek, B., … Rapaport, D. (2016). The cytosolic cochaperone Sti1 is relevant for mitochondrial biogenesis and morphology. *FEBS Journal*, *283*, 3338–3352. https://doi.org/10.1111/febs.13813

Huang, J.-D., Brady, S. T., Richards, B. W., Stenoien, D., Resau, J. H., Copeland, N. G., & Jenkins, N. A. (1999). Direct interaction of microtubule- and actin-based transport motors. *Nature*, *397*(6716), 267–270. https://doi.org/10.1038/16722

Jimah, J. R., & Hinshaw, J. E. (2019). Structural Insights into the Mechanism of Dynamin Superfamily Proteins. *Trends in Cell Biology*, *29*(3), 257–273. https://doi.org/10.1016/j.tcb.2018.11.003

Khodzhaeva, V., Schreiber, Y., Geisslinger, G., Brandes, R. P., Brüne, B., & Namgaladze, D. (2021). Mitofusin 2 Deficiency Causes Pro-Inflammatory Effects in Human Primary Macrophages. *Frontiers in Immunology*, *12*(August), 1–15. https://doi.org/10.3389/fimmu.2021.723683

Kijima, K., Numakura, C., Izumino, H., Umetsu, K., Nezu, A., Shiiki, T., … Hayasaka, K. (2005). Mitochondrial GTPase mitofusin 2 mutation in Charcot-Marie-Tooth neuropathy type 2A. *Human Genetics*, *116*(1–2), 23–27. https://doi.org/10.1007/s00439-004-1199-2

Kleele, T., Rey, T., Winter, J., Zaganelli, S., Mahecic, D., Perreten Lambert, H., … Manley, S. (2021). Distinct fission signatures predict mitochondrial degradation or biogenesis. *Nature*, *593*(7859), 435–439. https://doi.org/10.1038/s41586-021-03510-6

Leboucher, G. P., Tsai, Y. C., Yang, M., Shaw, K. C., Zhou, M., Veenstra, T. D., … Weissman, A. M. (2012). Stress-Induced Phosphorylation and Proteasomal Degradation of Mitofusin 2 Facilitates Mitochondrial Fragmentation and Apoptosis. *Molecular Cell*, *47*(4), 547–557. https://doi.org/10.1016/j.molcel.2012.05.041

Lee, J. Y., Kapur, M., Li, M., Choi, M. C., Choi, S., Kim, H. J., … Yao, T. P. (2014). MFN1 deacetylation activates adaptive mitochondrial fusion and protects metabolically challenged mitochondria. *Journal*

*of Cell Science*, *127*(22), 4954–4963. https://doi.org/10.1242/jcs.157321

Legros, Fréderic; Lombès, Anne; Frachon, Paule; Rojo, M. (2002). Mitochondrial Fusion in Human Cells Is Efficient, Requires the Inner Membrane Potential, and Is Mediated by Mitofusins. *Molecular Biology of the Cell*, *13*(November), 4100–4109. https://doi.org/10.1091/mbc.E02

Li, Y. J., Cao, Y. L., Feng, J. X., Qi, Y., Meng, S., Yang, J. F., … Gao, S. (2019). Structural insights of human mitofusin-2 into mitochondrial fusion and CMT2A onset. *Nature Communications*, *10*(1). https://doi.org/10.1038/s41467-019-12912-0

López-Doménech, G., Covill-Cooke, C., Ivankovic, D., Halff, E. F., Sheehan, D. F., Norkett, R., … Kittler, J. T. (2018). Miro proteins coordinate microtubule- and actin-dependent mitochondrial transport and distribution. *The EMBO Journal*, *37*(3), 321–336. https://doi.org/10.15252/embj.201696380

López-Doménech, G., Covill-Cooke, C., Ivankovic, D., Halff, E. F., Sheehan, D. F., Norkett, R., … Kittler, J. T. (2018). Miro proteins coordinate microtubule- and actin-dependent mitochondrial transport and distribution. *The EMBO Journal*, e96380. https://doi.org/10.15252/embj.201696380

Losó n, O. C., Song, Z., Chen, H., & Chan, D. C. (2013). Fis1, Mff, MiD49, and MiD51 mediate Drp1 recruitment in mitochondrial fission. *Molecular Biology of the Cell*, *24*(5), 659–667. https://doi.org/10.1091/mbc.E12-10-0721

Lundby, A., Andersen, M. N., Steffensen, A. B., Horn, H., Kelstrup, C. D., Francavilla, C., … Olsen, J. V. (2013). In vivo phosphoproteomics analysis reveals the cardiac targets of β-adrenergic receptor signaling. *Science Signaling*, *6*(278), rs11. https://doi.org/10.1126/scisignal.2003506

MacAskill, A. F., Brickley, K., Stephenson, F. A., & Kittler, J. T. (2009). GTPase dependent recruitment of Grif-1 by Miro1 regulates mitochondrial trafficking in hippocampal neurons. *Molecular and Cellular Neuroscience*, *40*(3), 301–312. https://doi.org/10.1016/j.mcn.2008.10.016

MacAskill, A. F., Rinholm, J. E., Twelvetrees, A. E., Arancibia-Carcamo, I. L., Muir, J., Fransson, A., … Kittler, J. T. (2009). Miro1 Is a Calcium Sensor for Glutamate Receptor-Dependent Localization of Mitochondria at Synapses. *Neuron*, *61*(4), 541–555. https://doi.org/10.1016/j.neuron.2009.01.030

Mandal, A., & Drerup, C. M. (2019). Axonal Transport and Mitochondrial Function in Neurons. *Frontiers in Cellular Neuroscience*, *13*(August), 1–11. https://doi.org/10.3389/fncel.2019.00373

Mehta, M. M., Weinberg, S. E., & Chandel, N. S. (2017). Mitochondrial control of immunity: Beyond ATP. *Nature Reviews Immunology*, *17*(10), 608–620. https://doi.org/10.1038/nri.2017.66

Mendis, D. A., Rosenberg, M., & Azam, F. (2022). Identification of Mfn2-S249 as a Phosphoregulatory Switch of Mitochondrial Fusion Dynamics. In *bioRxiv*.

Mishra, P., & Chan, D. C. (2014). Mitochondrial dynamics and inheritance during cell division, development and disease. *Nature Reviews Molecular Cell Biology*, *15*(10), 634–646. https://doi.org/10.1038/nrm3877

Misko, A., Jiang, S., Wegorzewska, I., Milbrandt, J., & Baloh, R. H. (2010). Mitofusin 2 is necessary for transport of axonal mitochondria and interacts with the Miro/Milton complex. *Journal of Neuroscience*, *30*(12), 4232–4240. https://doi.org/10.1523/JNEUROSCI.6248-09.2010

Misko, A. L., Sasaki, Y., Tuck, E., Milbrandt, J., & Baloh, R. H. (2012). Mitofusin2 mutations disrupt axonal mitochondrial positioning and promote axon degeneration. *Journal of Neuroscience*, *32*(12), 4145–4155. https://doi.org/10.1523/JNEUROSCI.6338-11.2012

Moore, A. S., & Holzbaur, E. L. (2018). Mitochondrial-cytoskeletal interactions: dynamic associations that facilitate network function and remodeling. *Current Opinion in Physiology*, *3*(Figure 1), 94–100. https://doi.org/10.1016/j.cophys.2018.03.003

Moore, A. S., Wong, Y. C., Simpson, C. L., & Holzbaur, E. L. F. (2016). Dynamic actin cycling through mitochondrial subpopulations locally regulates the fission-fusion balance within mitochondrial networks. *Nature Communications*, *7*(May 2015). https://doi.org/10.1038/ncomms12886

Morris, R. L., & Hollenbeck, P. J. (1993). The regulation of bidirectional mitochondrial transport is coordinated with axonal outgrowth. *Journal of Cell Science*, *104*(3), 917 LP – 927. Retrieved from http://jcs.biologists.org/content/104/3/917.abstract

Morris, R. L., & Hollenbeck, P. J. (1995). Axonal transport of mitochondria along microtubules and F-actin in living vertebrate neurons. *The Journal of Cell Biology*, *131*(5), 1315–1326. Retrieved from https://www.ncbi.nlm.nih.gov/pubmed/8522592

Narendra, D., Tanaka, A., Suen, D. F., & Youle, R. J. (2008). Parkin is recruited selectively to impaired mitochondria and promotes their autophagy. *Journal of Cell Biology*, *183*(5), 795–803. https://doi.org/10.1083/jcb.200809125

Nguyen, J. P., Shipley, F. B., Linder, A. N., Plummer, G. S., Liu, M., Setru, S. U., … Leifer, A. M. (2016). Whole-brain calcium imaging with cellular resolution in freely behaving Caenorhabditis elegans. *Proceedings of the National Academy of Sciences of the United States of America*, *113*(8), E1074–E1081. https://doi.org/10.1073/pnas.1507110112

Otera, H., Wang, C., Cleland, M. M., Setoguchi, K., Yokota, S., Youle, R. J., & Mihara, K. (2010). Mff is an essential factor for mitochondrial recruitment of Drp1 during mitochondrial fission in mammalian cells. *Journal of Cell Biology*, *191*(6), 1141–1158. https://doi.org/10.1083/jcb.201007152

Palmer, C. S., Osellame, L. D., Laine, D., Koutsopoulos, O. S., Frazier, A. E., & Ryan, M. T. (2011). MiD49 and MiD51, new components of the mitochondrial fission machinery. *EMBO Reports*, *12*(6), 565–573. https://doi.org/10.1038/embor.2011.54

Pathak, D., Sepp, K. J., & Hollenbeck, P. J. (2010). Evidence that myosin activity opposes microtubule-based axonal transport of mitochondria. *Journal of Neuroscience*, *30*(26), 8984–8992. https://doi.org/10.1523/JNEUROSCI.1621-10.2010

Pyakurel, A., Savoia, C., Hess, D., & Scorrano, L. (2015a). Extracellular Regulated Kinase Phosphorylates Mitofusin 1 to Control Mitochondrial Morphology and Apoptosis. *Molecular Cell*, *58*(2), 244–254. https://doi.org/10.1016/j.molcel.2015.02.021

Pyakurel, A., Savoia, C., Hess, D., & Scorrano, L. (2015b). Extracellular Regulated Kinase Phosphorylates Mitofusin 1 to Control Mitochondrial Morphology and Apoptosis. *Molecular Cell*, *58*(2), 244–254. https://doi.org/10.1016/j.molcel.2015.02.021

Quintero, O. A., DiVito, M. M., Adikes, R. C., Kortan, M. B., Case, L. B., Lier, A. J., … Cheney, R. E. (2009). Human Myo19 is a novel myosin that associates with mitochondria. *Current Biology : CB*, *19*(23), 2008–2013. https://doi.org/10.1016/j.cub.2009.10.026

Rambold, A. S., Kostelecky, B., Elia, N., & Lippincott-Schwartz, J. (2011). Tubular network formation protects mitochondria from autophagosomal degradation during nutrient starvation. *Proceedings of the National Academy of Sciences of the United States of America*, *108*(25), 10190–10195. https://doi.org/10.1073/pnas.1107402108

Rawson, R. L., Yam, L., Weimer, R. M., Bend, E. G., Hartwieg, E., Horvitz, H. R., … Jorgensen, E. M. (2014). Axons degenerate in the absence of mitochondria in C. elegans. *Current Biology*, *24*(7), 760–765. https://doi.org/10.1016/j.cub.2014.02.025

Rodríguez-Pérez, F., Manford, A. G., Pogson, A., Ingersoll, A. J., Martínez-González, B., & Rape, M. (2021). Ubiquitin-dependent remodeling of the actin cytoskeleton drives cell fusion. *Developmental Cell*, *56*(5), 588-601.e9. https://doi.org/10.1016/j.devcel.2021.01.016

Rohn, J. L., Patel, J. V., Neumann, B., Bulkescher, J., McHedlishvili, N., McMullan, R. C., … Baum, B. (2014). Myo19 ensures symmetric partitioning of mitochondria and coupling of mitochondrial segregation to cell division. *Current Biology*, *24*(21), 2598–2605. https://doi.org/10.1016/j.cub.2014.09.045

Rojo, M., Legros, F., Chateau, D., & Lombès, A. (2002). Membrane topology and mitochondrial targeting of mitofusins, ubiquitous mammalian homologs of the transmembrane GTPase Fzo. *Journal of Cell Science*, *115*(8), 1663–1674. https://doi.org/10.1242/jcs.115.8.1663

Russo, G. J., Louie, K., Wellington, A., Macleod, G. T., Hu, F., Panchumarthi, S., & Zinsmaier, K. E. (2009). Drosophila Miro is required for both anterograde and retrograde axonal mitochondrial transport. *Journal of Neuroscience*, *29*(17), 5443–5455. https://doi.org/10.1523/JNEUROSCI.5417-08.2009

Ruthel, G., & Hollenbeck, P. J. (2003). Response of Mitochondrial Traffic to Axon Determination and Differential Branch Growth. *The Journal of Neuroscience*, *23*(24), 8618 LP – 8624. https://doi.org/10.1523/JNEUROSCI.23-24-08618.2003

Samanas, N. B., Engelhart, E. A., & Hoppins, S. (2020). Defective nucleotide-dependent assembly and membrane fusion in Mfn2 CMT2A variants improved by Bax. *Life Science Alliance*, *3*(5), 1–11. https://doi.org/10.26508/lsa.201900527

Saotome, M., Safiulina, D., Szabadkai, G., Das, S., Fransson, Å., Aspenstrom, P., … Hajnóczky, G. (2008). Bidirectional Ca2+-dependent control of mitochondrial dynamics by the Miro GTPase. *Proceedings of the National Academy of Sciences of the United States of America*, *105*(52), 20728–20733. https://doi.org/10.1073/pnas.0808953105

Schnapp, B. J., & Reese, T. S. (1989). Dynein is the motor for retrograde axonal transport of organelles. *Proceedings of the National Academy of Sciences*, *86*(5), 1548 LP – 1552. https://doi.org/10.1073/pnas.86.5.1548

Schuler, M. H., Lewandowska, A., Di Caprio, G., Skillern, W., Upadhyayula, S., Kirchhausen, T., … Cunniff, B. (2017). Miro1-mediated mitochondrial positioning shapes intracellular energy gradients required for cell migration. *Molecular Biology of the Cell*, *28*(16), 2159–2169. https://doi.org/10.1091/mbc.E16-10-0741

Sebastián, D., Hernández-Alvarez, M. I., Segalés, J., Sorianello, E., Muñoz, J. P., Sala, D., … Zorzano, A. (2012). Mitofusin 2 (Mfn2) links mitochondrial and endoplasmic reticulum function with insulin signaling and is essential for normal glucose homeostasis. *Proceedings of the National Academy of Sciences of the United States of America*, *109*(14), 5523–5528. https://doi.org/10.1073/pnas.1108220109

Shutt, T., Geoffrion, M., Milne, R., & McBride, H. M. (2012). The intracellular redox state is a core determinant of mitochondrial fusion. *EMBO Reports*, *13*(10), 909–915. https://doi.org/10.1038/embor.2012.128

Sloat, S. R., Whitley, B. N., Engelhart, E. A., & Hoppins, S. (2019). Identification of a mitofusin specificity region that confers unique activities to Mfn1 and Mfn2. *Molecular Biology of the Cell*, *30*(17), 2309–2319. https://doi.org/10.1091/mbc.E19-05-0291

Sloat, Stephanie R., & Hoppins, S. (2023). A dominant negative mitofusin causes mitochondrial perinuclear clusters because of aberrant tethering. *Life Science Alliance*, *6*(1), 1–17. https://doi.org/10.26508/lsa.202101305

Sloat, Stephanie R, & Hoppins, S. (2022). *A dominant negative mitofusin causes mitochondrial perinuclear clusters because of aberrant tethering*. *6*(1), 1–17. https://doi.org/10.26508/lsa.202101305

Soh, M. S., Cheng, X., Vijayaraghavan, T., Vernon, A., Liu, J., & Neumann, B. (2020). Disruption of genes associated with Charcot-Marie-Tooth type 2 lead to common behavioural, cellular and molecular defects in Caenorhabditis elegans. *PLoS ONE*, *15*(4), 1–29. https://doi.org/10.1371/journal.pone.0231600

Stowers, R. S., Megeath, L. J., Górska-Andrzejak, J., Meinertzhagen, I. A., & Schwarz, T. L. (2002). Axonal transport of mitochondria to synapses depends on milton, a novel Drosophila protein. *Neuron*, *36*(6), 1063–1077. https://doi.org/10.1016/S0896-6273(02)01094-2

Sure, G. R., Chatterjee, A., Mishra, N., Sabharwal, V., Devireddy, S., Awasthi, A., … Koushika, S. P. (2018). UNC-16/JIP3 and UNC-76/FEZ1 limit the density of mitochondria in C. elegans neurons by maintaining the balance of anterograde and retrograde mitochondrial transport. *Scientific Reports*, *8*(1), 1–12. https://doi.org/10.1038/s41598-018-27211-9

Taguchi, N., Ishihara, N., Jofuku, A., Oka, T., & Mihara, K. (2007). Mitotic phosphorylation of dynamin-related GTPase Drp1 participates in mitochondrial fission. *Journal of Biological Chemistry*, *282*(15), 11521–11529. https://doi.org/10.1074/jbc.M607279200

Tanaka, K., Sugiura, Y., Ichishita, R., Mihara, K., & Oka, T. (2011). KLP6: A newly identified kinesin that regulates the morphology and transport of mitochondria in neuronal cells. *Journal of Cell Science*,

*124*(14), 2457–2465. https://doi.org/10.1242/jcs.086470

Tanaka, Y., Kanai, Y., Okada, Y., Nonaka, S., Takeda, S., Harada, A., & Hirokawa, N. (1998). Targeted disruption of mouse conventional kinesin heavy chain, kif5B, results in abnormal perinuclear clustering of mitochondria. *Cell*, *93*(7), 1147–1158. https://doi.org/10.1016/s0092-8674(00)81459-2

Tondera, D., Grandemange, S., Jourdain, A., Karbowski, M., Mattenberger, Y., Herzig, S., … Martinou, J. C. (2009). SlP-2 is required for stress-induced mitochondrial hyperfusion. *EMBO Journal*, *28*(11), 1589–1600. https://doi.org/10.1038/emboj.2009.89

Toyama, E. Q., Herzig, S., Courchet, J., Lewis, T. L., Losón, O. C., Hellberg, K., … Shaw, R. J. (2016). AMP-activated protein kinase mediates mitochondrial fission in response to energy stress. *Science*, *351*(6270), 275–281. https://doi.org/10.1126/science.aab4138

van Spronsen, M., Mikhaylova, M., Lipka, J., Schlager, M. A., van den Heuvel, D. J., Kuijpers, M., … Hoogenraad, C. C. (2013). TRAK/Milton Motor-Adaptor Proteins Steer Mitochondrial Trafficking to Axons and Dendrites. *Neuron*, *77*(3), 485–502. https://doi.org/10.1016/j.neuron.2012.11.027

Verburg, J., & Hollenbeck, P. J. (2008). Mitochondrial membrane potential in axons increases with local nerve growth factor or semaphorin signaling. *The Journal of Neuroscience : The Official Journal of the Society for Neuroscience*, *28*(33), 8306–8315. https://doi.org/10.1523/JNEUROSCI.2614-08.2008

Vives-Bauza, C., Zhou, C., Huang, Y., Cui, M., De Vries, R. L. A., Kim, J., … Przedborski, S. (2010). PINK1-dependent recruitment of Parkin to mitochondria in mitophagy. *Proceedings of the National Academy of Sciences of the United States of America*, *107*(1), 378–383. https://doi.org/10.1073/pnas.0911187107

Wada, T., & Penninger, J. M. (2004). Mitogen-activated protein kinases in apoptosis regulation. *Oncogene*, *23*(16 REV. ISS. 2), 2838–2849. https://doi.org/10.1038/sj.onc.1207556

Waterston, R., Thompson, O., Edgley, M., Strasbourger, P., Flibotte, S., Ewing, B., … Moerman, D. (2013). The Million Mutation Project: A new approach to genetics in Caenorhabditis elegans. *Genome Research*, 1749–1762. https://doi.org/10.1101/gr.157651.113.Freely

Whitley, B. N. (2019). *Characterizing the molecular mechanisms of mitochondrial fusion and division in healthy and diseased cells*. University of Washington.

Yan, L., Qi, Y., Huang, X., Yu, C., Lan, L., Guo, X., … Lou, Z. (2018). Structural basis for GTP hydrolysis and conformational change of MFN1 in mediating membrane fusion. *Nature Structural and Molecular Biology*, *25*(3), 233–243. https://doi.org/10.1038/s41594-018-0034-8

Yang, Y., Ouyang, Y., Yang, L., Beal, M. F., McQuibban, A., Vogel, H., & Lu, B. (2008). Pink1 regulates mitochondrial dynamics through interaction with the fission/fusion machinery. *Proceedings of the National Academy of Sciences of the United States of America*, *105*(19), 7070–7075. https://doi.org/10.1073/pnas.0711845105

You, M. H., Jeon, M. J., Kim, S. ryeong, Lee, W. K., Cheng, S. yann, Jang, G., … Kim, W. G. (2021). Mitofusin-2 modulates the epithelial to mesenchymal transition in thyroid cancer progression.

*Scientific Reports*, *11*(1), 1–12. https://doi.org/10.1038/s41598-021-81469-0

Zervopoulos, S. D., Boukouris, A. E., Saleme, B., Haromy, A., Tejay, S., Sutendra, G., & Michelakis, E. D. (2022). MFN2-driven mitochondria-to-nucleus tethering allows a non-canonical nuclear entry pathway of the mitochondrial pyruvate dehydrogenase complex. *Molecular Cell*, *82*(5), 1066-1077.e7. https://doi.org/10.1016/j.molcel.2022.02.003

Zhao, Y., Song, E., Wang, W., Hsieh, C. H., Wang, X., Feng, W., … Shen, K. (2021). Metaxins are core components of mitochondrial transport adaptor complexes. *Nature Communications*, *12*(1). https://doi.org/10.1038/s41467-020-20346-2

Zheng, H., Li, Q., Li, S., Li, Z., Brotto, M., Weiss, D., … Qu, C. K. (2023). Loss of Ptpmt1 limits mitochondrial utilization of carbohydrates and leads to muscle atrophy and heart failure in tissue-specific knockout mice. *ELife*, *12*, 1–23. https://doi.org/10.7554/eLife.86944

Zhou, W., Chen, K.-H., Cao, W., Zeng, J., Liao, H., Zhao, L., & Guo, X. (2010). Mutation of the protein kinase A phosphorylation site influences the anti-proliferative activity of mitofusin 2. *Atherosclerosis*, *211*(1), 216–223. https://doi.org/10.1016/j.atherosclerosis.2010.02.012